

Journal Pre-proofs

Coastal flood risks in China through the 21st century – An application of DIVA

Jiayi Fang, Daniel Lincke, Sally Brown, Robert J. Nicholls, Claudia Wolff, Jan-Ludolf Merkmens, Jochen Hinkel, Athanasios T. Vafeidis, Peijun Shi, Min Liu

PII: S0048-9697(19)35303-3
DOI: <https://doi.org/10.1016/j.scitotenv.2019.135311>
Reference: STOTEN 135311

To appear in: *Science of the Total Environment*

Received Date: 26 July 2019
Revised Date: 11 October 2019
Accepted Date: 29 October 2019



Please cite this article as: J. Fang, D. Lincke, S. Brown, R.J. Nicholls, C. Wolff, J-L. Merkmens, J. Hinkel, A.T. Vafeidis, P. Shi, M. Liu, Coastal flood risks in China through the 21st century – An application of DIVA, *Science of the Total Environment* (2019), doi: <https://doi.org/10.1016/j.scitotenv.2019.135311>

This is a PDF file of an article that has undergone enhancements after acceptance, such as the addition of a cover page and metadata, and formatting for readability, but it is not yet the definitive version of record. This version will undergo additional copyediting, typesetting and review before it is published in its final form, but we are providing this version to give early visibility of the article. Please note that, during the production process, errors may be discovered which could affect the content, and all legal disclaimers that apply to the journal pertain.

© 2019 Elsevier B.V. All rights reserved.

Coastal flood risks in China through the 21st century

– An application of DIVA

Jiayi Fang^{1,2,3}, Daniel Lincke⁴, Sally Brown^{3,5}, Robert J. Nicholls^{3,6}, Claudia Wolff⁷,
Jan-Ludolf Merkmens⁷, Jochen Hinkel^{4,8}, Athanasios T. Vafeidis⁷, Peijun Shi^{2,9*}, Min

Liu¹

1. Key Laboratory of Geographic Information Science, Ministry of Education, School of Geographic Sciences, East China Normal University, Shanghai 200241, China
2. Academy of Disaster Reduction and Emergency Management, Ministry of Emergency Management & Ministry of Education, Beijing 100875, China
3. School of Engineering, University of Southampton, Highfield Campus, Southampton, SO17 1BJ, UK
4. Global Climate Forum, 10178 Berlin, Germany
5. Department of Life and Environmental Sciences, Bournemouth University, Fern Barrow, Bournemouth. BH12 5BB. UK
6. Tyndall Centre for Climate Change Research, University of East Anglia, Norwich Research Park, Norwich NR4 7TJ
7. Coastal Risks and Sea-Level Rise Research Group, Department of Geography, Christian-Albrechts-University Kiel, Kiel, Germany
8. Division of Resource Economics, Albrecht Daniel Thaer-Institute and Berlin Workshop in Institutional Analysis of Social-Ecological Systems (WINS), Humboldt-University, 10099 Berlin, Germany
9. School of Geographical Science, Qinghai Normal University, Xining 810016, China

*Corresponding author: Prof. Peijun Shi (E-mail: spj@bnu.edu.cn)

Abbreviations

AW3D30: ALOS Global Digital Surface Model World 3D—30 m

DEM: Digital Elevation Model

DIVA: Dynamic Interactive Vulnerability Assessment

ESL: Extreme sea level

GADM: Global Administrative Areas

GCM: General Circulation Model

GDP: Gross Domestic Product

GPCN: Grid Population Dataset of China

GTSR: Global Tide and Surge Reanalysis

LECZ: Low Elevation Coastal Zone

RCP: Representative Concentration Pathways

SLR: Sea level rise

SSP: Shared Socioeconomic Pathways

Abstract

China experiences frequent coastal flooding, with nearly US\$ 77 billion of direct economic losses and over 7,000 fatalities reported from 1989 to 2014. Flood damages are likely to grow due to climate change induced sea-level rise and increasing exposure if no further adaptation measures are taken. This paper quantifies potential damage and adaptation costs of coastal flooding in China over the 21st Century, including the effects of sea-level rise. It develops and utilises a new, detailed coastal database of China developed within the Dynamic Interactive Vulnerability Assessment (DIVA) model framework. The refined database provides a more realistic spatial representation of coasts, with more than 2,700 coastal segments, covering 28,966 km of coastline. Over 50% of China's coast is artificial, representing defended coast and/or claimed land. Coastal flood damage and adaptation costs for China are assessed for different Representative Concentration Pathway (RCP) and Shared Socio-economic Pathways (SSP) combinations representing climate change and socio-economic change and two adaptation strategies: no upgrade of currently existing defences and maintaining current protection levels. By 2100, 0.7-20.0 million people may be flooded/yr and US\$ 67-3,308 billion damages/yr are projected without upgrade to defences. In contrast, maintaining the current protection level would reduce those numbers to 0.2-0.4 million people flooded/yr and US\$ 22-60 billion/yr flood costs by 2100, with a protection investment costs of US\$ 8-17 billion/yr. In 2100, maintaining current protection levels, dikes costs are two orders of magnitude smaller than flood costs across all scenarios, even without accounting for indirect

damages. This research improves on earlier national assessments of China by generating a wider range of projections, based on improved datasets. The information delivered in this study will help governments, policy-makers, insurance companies and local communities in China understand risks and design appropriate strategies to adapt to increasing coastal flood risk in an uncertain world.

Keywords: Coastal flooding, sea level rise, risk assessment, climate change impacts, China

1 Introduction

Coastal areas are threatened by extreme weather events and climate change. Coastal floods caused by extreme sea levels (ESLs) due to combined high tide and storm surges are one of the most serious risks, which impact upon society, the economy and the wider natural environment. Sea level rise (SLR) further exacerbates this risk over time (Nicholls, 2004; Hanson et al., 2011; Hallegatte et al., 2013; Nicholls et al., 2014; Hinkel et al., 2014).

Coastal areas in China are important population and economic centres and are prone to natural disasters, especially for flood disasters (Hu et al., 2018). Coastal China comprises 14 provincial-level administrative regions which encompasses a wide latitudinal range from Liaodong Bay (at 41° N) to the South China Sea (at 4° N), including one autonomous region: Guangxi; two municipalities: Shanghai and Tianjin; three Special Administrative Region: Taiwan, Hong Kong and Macao; eight provinces from north to south: Liaoning, Hebei, Shandong, Jiangsu, Zhejiang, Fujian,

Guangdong and Hainan. More than 40% of the population lives in coastal provincial administrative regions, which contribute nearly 60% of the national gross domestic product (GDP). About 47% of the national capital stock was found in the Eastern Economic Region¹ in 2012 (Wu et al. 2014). Coastal population and assets in China are growing much faster than in inland areas (Seto, 2011). It is expected that this trend and related coastal infrastructure development and maritime activities will continue with the proposal of China's 21st Century Maritime Silk Road programme (Liu, 2014). However, these areas also experience frequent storm surges and coastal flooding which caused approximately US\$ 77 billion direct economic losses and more than 7,000 fatalities from 1989 to 2014 (Fang et al., 2017). Additionally, rapid urbanization has led to a sharp increase of exposure in coastal areas in China and has been accompanied by groundwater pumping causing subsidence, plus an expanding impermeable urban area. These risks are likely to grow due to climate change and increasing exposure if no further adaptation measures are taken.

Given this situation, it is crucial to analyse the future impacts of coastal flooding in China under a range of sea-level rise and socio-economic change scenarios; and also consider how adaptation could alter these impacts. This information will inform the long-term planning of development of the coastal zone of China. To our knowledge, a number of studies have considered sea-level rise in China (e.g., Han et al., 1995), or sea-level rise in parts of China (e.g., Wang et al., 1995; Huang et al., 2004; Kang et al.,

¹Eastern Economic Region consists of Hebei, Beijing, Tianjin, Shandong, Jiangsu, Shanghai, Zhejiang, Fujian, Guangdong and Hainan. Except Beijing, other are coastal provincial administrative regions.

2016; Wang et al., 2018), but there is no quantitative national coastal flood impact assessment. This paper fills this gap by including improved coastal datasets and considering demographic and economic scenarios and coastal protection strategies.

The aim of this study is to investigate the coastal flood damage and adaptation costs across China by considering three Representative Concentration Pathways (RCP) and Shared Socio-economic Pathways (SSP) combinations representing climate change and socio-economic change, respectively, as well as considering two adaptation strategies. This is achieved by two objectives: 1) to generate a new and high-resolution coastal database for China; and 2) to assess potential coastal flood risks under the different scenarios and adaptation strategies.

Hinkel et al. (2014) conducted a global assessment of coastal flood risk, including China, using the Dynamic Interactive Vulnerability Assessment (DIVA) modelling framework. The original DIVA database was developed for global assessment (Vafeidis et al., 2008), and includes 226 segments covering 12,288 km of coastline in China. The official coastal length in China is about 18,000 km for the continental coast (Wang, 1980). A major constraint on coastal flood risk assessment at national scale is the data availability and quality (Nicholls et al., 2008). Therefore, when new datasets emerge, it is important to make the most of these in future analysis. For example, Wolff et al. (2016) suggest that a more refined segmentation using updated data within the DIVA modelling framework can improve coastal flood risk assessment. Hence, a new and more detailed coastal database is developed for China and linked to the DIVA algorithms for a national assessment.

The paper is structured as follows. Section 2 describes materials and methods used to build the new and high-resolution coastal database of China. Section 3 shows the results and discussion of coastal flood risk by considering various dimensions. Conclusions are presented in Section 4.

2 Materials and methods

We use the DIVA coastal flooding module, as presented in Hinkel et al. (2014), to calculate coastal flood risks in China. DIVA is an integrated, state-of-the-art research model of coastal systems that assesses biophysical and socio-economic consequences of sea-level rise, socio-economic development and adaptation (Hinkel and Klein, 2009). Changes in sea-level are represented by the RCPs (van Vuuren et al., 2011). In this case, regional sea-level rise scenarios were used. Future coastal population exposure changes are computed from SSPs (IIASA, 2012; O'Neill et al., 2014). Adaptation is an explicit element of the DIVA framework. Within DIVA, the algorithms and database are separated, where the latter is based on a linear segmentation of the coast (Vafeidis et al., 2008).

Figure 1 summarises the methodology, which consists of three main steps. The first step is to improve the quality and resolution of the spatial assessment units by using a more detailed coastline and segmentation process (as discussed in Section 2.1). The second step is to calculate exposure using elevation and population datasets, and to create a data structure that enables the model to run (see Section 2.2). Last, the DIVA

coastal flooding module is used to assess future coastal flood risks for different scenarios and adaptation strategies (see Section 2.3).

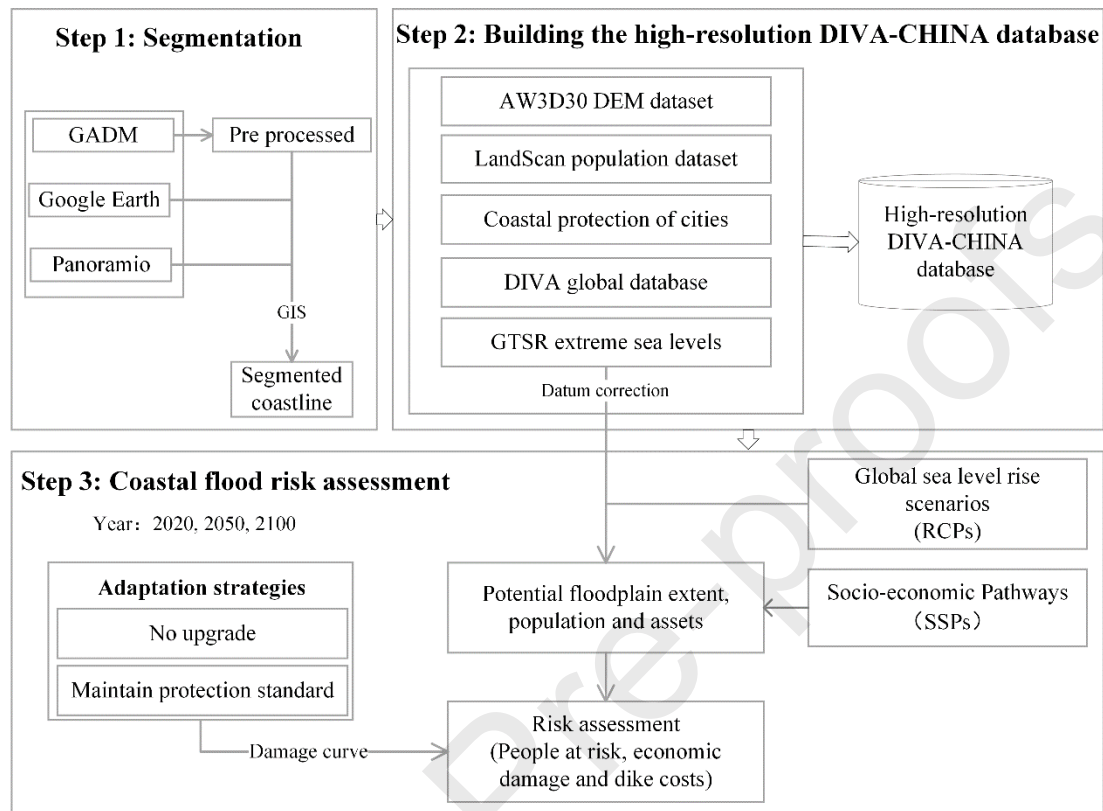


Fig. 1 Flowchart showing the general methodological approach by dividing into three steps.

2.1 Segmentation

The DIVA model operates on data attributed to coastline segments. As the resolution of the Chinese coastline in the global database is rather coarse, a refined version was developed for this study. To downscale the segmentation and the coastal database for China, we generated a larger number of segments and populated the database with local-level datasets, following similar approaches to those used in McFadden et al. (2007) and Wolff et al. (2016; 2018) (Supplementary Fig. S1). Each segment associated with a range of geophysical, ecology, economic and demographic

information, reflects a uniform changing response or sequence of responses within the coastal system, and subsequent modelling and analysis are based on these segments.

The coastline acts as a base layer for all the following steps and hence plays a fundamental role in the analysis. After reviewing several possible coastlines, we selected the coastline from Global Administrative Areas (GADM) (Supplementary Tab. S1) and pre-processed and transformed the data following Wolff et al. (2018). Then urban and rural coasts have been identified based on the interpretation of satellite imagery and an urban extent dataset (Huang et al., 2015; Xu et al., 2016). Urban areas are defined with a predominantly impervious surface environment, such as buildings and roads. Classification were based on visual interpretation of Google imagery and urban extent dataset. Due to the lack of a national coastal geomorphic characteristics dataset for coastal China, an independent consistent dataset was generated with Google Earth and photos from the web-service “Panoramio” (<http://www.panoramio.com/>). Panoramio provides location-tagged photographs for the whole study area and gave a good impression of the type of coast, which has been used to monitor changes of coastlines as an assistant tool (Scheffers et al., 2012). The geomorphic coastal type data was then compiled based on the visual inspection from the available satellite imagery as well as geographically tagged photos. Adjusted from Wolff et al. (2016), in this study, the coastlines were classified into five main types: 1) sandy, 2) rocky (unerodible or limited erodible), 3) muddy, 4) artificial and 5) river mouth (Supplementary Tab. S2). Using this as a base layer, the coastline segmentation was performed within a GIS. The coastline was split every time the type

of coast differed based on the satellite data and photographs or a political boundary was crossed.

2.2 Building the high-resolution DIVA-China database

To build the refined database, we recalculate exposure at different elevation increments using baseline elevation and population datasets; we also update coastal protection data, extreme sea levels as well as parameters from the DIVA global dataset.

To assess coastal exposure to inundation, the bathtub approach is employed, which is widely used for macro-scale analysis (e.g. Kebede et al., 2012; Hallegatte et al., 2013). The hydrological connectivity (8 neighbour cells) is also considered when calculating the inundated area within the bathtub approach (Li et al., 2009). The free-downloaded Digital Elevation Models (DEMs) ALOS Global Digital Surface Model (ALOS World 3D—30 m, AW3D30 for short) is employed. AW3D30 with a spatial resolution of 1 arcsec (approx. 30 m) and a vertical resolution of 1 m (Tadono et al., 2016). The dataset is published based on the global digital surface model dataset (5-meter mesh version) of the ‘World 3D Topographic Data’ which is one of the most precise global-scale elevation datasets at this time (Courtya et al., 2017; Hu et al., 2017). The population count datasets of LandScan have been used to calculate the exposed population. The dataset is with a resolution of 30 arcsec (approx. 1 km) and is with base year of 2010 (Bright et al., 2011).

There is no empirical data on actual protection levels of China in the global DIVA database. Thus, we use flood protection data of coastal cities in China from various

sources (Supplementary Tab. S3). This table provides flood protection standard by return period. For those coastal cities without protection data, we follow the National Standard for Flood Control of China (2014) to estimate the flood protection standard. The standard requires that cities with permanent resident population of more than 1.5 million people are equipped with at least 200-year return period flood protection facilities (Supplementary Tab. S4). The protection information is attached to the segments of those population centres that have been identified in the segmentation.

Extreme water levels given for different return periods utilised in this study are from the first global reanalysis of storm surges and extreme sea levels (GTSR) based on hydrodynamic modelling (Muis et al., 2016). GTSR consists of time series of tides and surges, and estimates of extreme sea levels. The extreme water levels have been datum corrected to the same datum as the DEM used in DIVA.

Other basic information used in DIVA (e.g. GDP per capita of China) has been updated from the base year of 1995 to a baseline in 2010. For example, based on recent coastal projects construction in China, the cost of seawall construction was US\$3.4 million/km/m (Ke, 2014). The DIVA database for China is compiled by using similar approaches which can be found in Vafeidis et al. (2008).

2.3 Coastal flood risk assessment

The coastal flooding module in DIVA (version 5.0.0) was used to assess coastal flood risks in China. Local relative sea-level change is computed by adding regionalised climate-induced sea-level rise scenarios with glacial isostatic adjustment data

(Peltier,2000). In addition, for segments located in river deltas a subsidence rate of 2 mm/yr was assumed (following Hinkel et al., 2014).

Population and assets exposure to coastal flood events are computed using cumulative population and asset exposure functions. The estimation of the value of assets on a given elevation increment is undertaken by multiplying the population count with the local GDP per capita (province level) and an empirically estimated GDP-to-assets ratio of 2.8 taken from Hallegatte et al. (2013). We assume that when the water level is below the protection standard, people and assets are protected, and thus the loss is zero. For people, if there is no protection or the extreme water level is higher than the protection standard, the damage function is identical to the cumulative exposure function. In contrast for assets we assume a logistic depth-damage function (giving the fraction of assets damaged for a given flood depth) with a 2-m flood destroying 50% of the assets (Messner et al., 2007; Yin et al., 2012; Fig. 2). A more detailed description of the coastal flooding module in this study is presented in Hinkel et al. (2014).

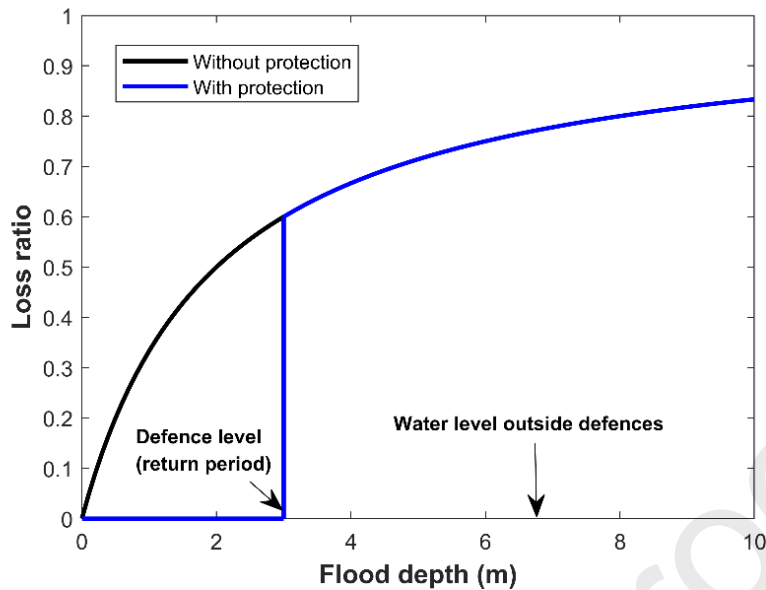


Fig. 2 Damage curve for the assessment of assets in the DIVA flood module (Blue line shows an example of a 3 m of defence, the loss ratio over 3 m is same as without protection).

The following parameters of coastal flooding are analysed in this study:

- 1) Exposure of the 100-year return period flood event: floodplain area extent (km^2), exposed population (million) and assets (billion US\$) (ignoring dikes);
- 2) Expected number of people flooded per year (million/yr);
- 3) Expected average annual flood costs (in billion US\$/yr);
- 4) Expected average annual dike costs comprise capital costs of building and upgrading dikes, as well as dike maintenance costs (in billion US\$/yr).

Adaptation is modelled by dikes, which is consistent with current practice in China where dikes are widely used (Ma et al., 2014). There are two protection strategies: (1) maintain protection standard (2010), and (2) no upgrade of currently existing defences.

Maintain protection standard means that dikes are kept at the current protection standard and thus raised over time with relative sea-level rise to against same degree of ESL. No upgrade means that dikes are kept at 2010 heights and not raised and thus

become increasingly less effective as sea levels rise. The protection standard does not change, even if socio-economic conditions change.

Future potential impacts in DIVA are assessed by taking sea-level rise and socioeconomic development scenarios into account. Following the work of Hinkel et al (2014), we used sea-level rise scenarios derived from three RCPs (RCP2.6, 4.5, and 8.5), four general circulation models (GCMs) (HadGEM2-ES, IPSL-CM5A-LR, MIROC-ESM-CHEM, and NorESM1-M) and three land-ice scenarios (low, medium and high). A more detailed description of these sea-level rise scenarios can be found in Hinkel et al. (2014). The projected relative sea-level rise along coastal China at the end of this century ranges from 21 cm to 119 cm with respect to the 1985-2005 mean across all GCMs and emission scenarios. The median value in 2100 for RCP2.6 is 38 cm, for RCP4.5 55 cm and for RCP8.5 85 cm (Fig. 3a; Supplementary Tab. S5).

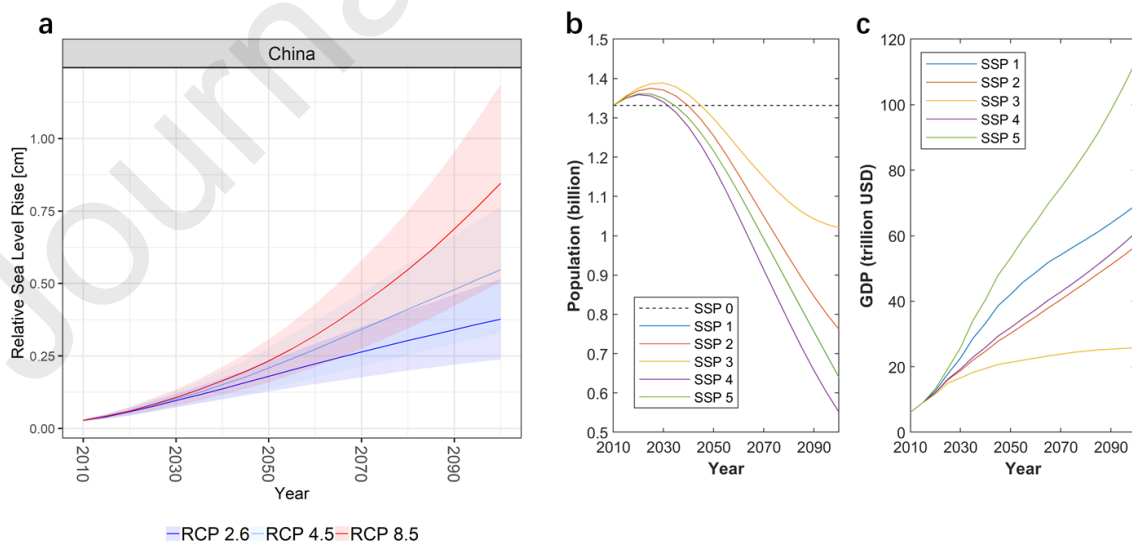


Fig. 3 a) The mean relative sea-level rise for China under sea-level rise scenarios (reference period: 1985-2005; Lines refer to median values, and shades areas show ranges of maximum and minimum values); b) Population (SSP5 overlays SSP1 for

population, SSP0 only refers to no change of population); c) GDP of China for socioeconomic scenarios from 2010 to 2100.

We utilise the SSPs to account for socioeconomic development. The SSPs provide five pathways of socioeconomic development (SSPs 1-5) including projections on population (Samir, K.C. and Lutz, W., 2017) and GDP (Leimbach et al., 2017). For this study, we assume homogeneous growth patterns and apply the national projections of population and GDP under each SSP to the segment to calculate future exposure. According to mean global total fertility rate, China is a low-fertility country (Samir and Lutz, 2017). SSP1 assumes sustainable development with emphasis on education, medical service and renewables, low fertility, low mortality and medium migration; SSP2 is moderate development, with medium fertility, mortality and migration. SSP3 is with high population growth and mortality, as well as low migration. SSP4 indicates low fertility and high mortality. In the SSP5 storyline, there is rapid economic development heavily based on fossil-fuel, with low capacity in the mitigation challenges (Samir and Lutz, 2014). Thus, the population projections for China will increase from 2010 to 2030, peaking at nearly 1.4 billion populations, then decreasing until the end of this century across all five SSPs scenarios (Fig. 3b). The trajectories are similar for the five SSPs until around 2030. Substantial difference occurs after then, with highest population in SSP3 (~1.0 billion) and the lowest in SSP4 (~0.6 billion) in 2100. As population decline in China is significant in all scenarios, an additional set of runs with constant (2010) population (SSP0) is included to demonstrate the changes due to climate change without demographic changes. The population of SSP0 is higher than the other five SSPs after 2035. The GDP increases

for the five SSP scenarios until 2100. The highest GDP is SSP5 (~US\$113 trillion) and the lowest is SSP3 (~US\$26 trillion) (Fig. 3b) in 2100.

Based upon the three RCP scenarios and five SSP scenarios, we generate a 3×5 matrix of core scenarios. We note that some RCP-SSP combinations (e.g., RCP2.6-SSP3) are unlikely to arise in practice (van Vuuren and Carter, 2014). Three plausible SSP and RCP combinations provide the basis for the analysis of future coastal flooding risks here, namely, RCP2.6-SSP1, RCP4.5-SSP2, and RCP8.5-SSP5 (Vousdoukas et al., 2018). RCP2.6-SSP1 describes a low greenhouse gas emission scenario and sustainable development scenario. RCP4.5-SSP2 indicates a moderate development pathway with moderate greenhouse gas emissions and development. RCP8.5-SSP5 refers to a world with fossil-fuel based development. In order to quantify relative contribution of climate and population on exposure (as described in Section 3.2), we adopt the method from Jones et al. (2015) and Liao et al. (2019). We decompose the change of population exposure into three effects, i.e., climate effect, population effect and joint change effect.

$$\Delta E = E_j - E_i = P_j \times C_j - P_i \times C_i = P_i \times \Delta C + C_i \times \Delta P + \Delta C \times \Delta P \quad (1)$$

To consider relative contribution of the factors compared with the population exposure in the base year, the percentage of the total change was considered (as used in Fig 6). This is noted in Equation 2, which was then multiplied by 100 to give a percentage.

$$\frac{\Delta E}{E_1} = \frac{P_i \times \Delta C + C_i \times \Delta P + \Delta C \times \Delta P}{P_i \times C_i} = \frac{\Delta C}{C_i} + \frac{\Delta P}{P_i} + \frac{\Delta P \Delta C}{P_i C_i} \quad (2)$$

In this equations, ΔE is the total change in population exposure, E_i is population exposure in base year, E_j is population exposure in target year. C_i and P_i are exposed areas which is dominant by SLR and population in base year, C_j and P_j are exposed areas and population in target year, and ΔC and ΔP are the change in exposed areas which is dominant by SLR and population from base year to target year. Here we refer to $C_i \times \Delta P$ as the population effect, $P_i \times \Delta C$ as the climate effect and $\Delta C \times \Delta P$ as the joint change effect.

3 Results and discussion

3.1 DIVA-China database

The new Chinese coastline segmentation produces 2,760 variable-length segments with maximum segment length of 99.99 km and minimum length of 0.11 km. The average segment length is 10.50 km. Compared with the global DIVA database, this is a 10-fold increase in the number of segments, which results in a 136% increase in coastline length from 12,288 km to 28,966 km (Tab. 1). The main reason for the increased coastline length is due to the inclusion of nearshore small islands (e.g. Zhoushan Islands in Zhejiang Province) (Supplementary Fig. S2), as previous studies were mainly based on continental coastlines.

The coastline of China has undergone rapid changes in the last 100 years due to natural factors (e.g. sediment supply) as well as anthropogenic influence (e.g. construction of dams in the catchments, dikes, land claim and other engineering structures) (Wang and Aubrey, 1987). Based on the high-resolution segmentation,

rocky coast accounts for 9,577 km or 33% of the total coastline. It is mainly distributed in small islands of Liaodong Peninsula, Zhejiang, Fujian, Guangdong and Taiwan provinces. Zhejiang and Fujian have the longest rocky coasts, at 2135 and 2183 km including small islands, respectively, accounting for 35% and 43% of the total length of the province (Tab. 1).

Tab. 1 Length of China's coastline according to the coastal typology classification based on the high-resolution segmentation.

Coastal type	Coastline (km)	Percent (%)
Sandy	2703	9.3
Rocky	9577	33.0
Muddy	1722	6.0
Artificial coasts	14828	51.2
River mouth	137	0.5
Total	28967	100

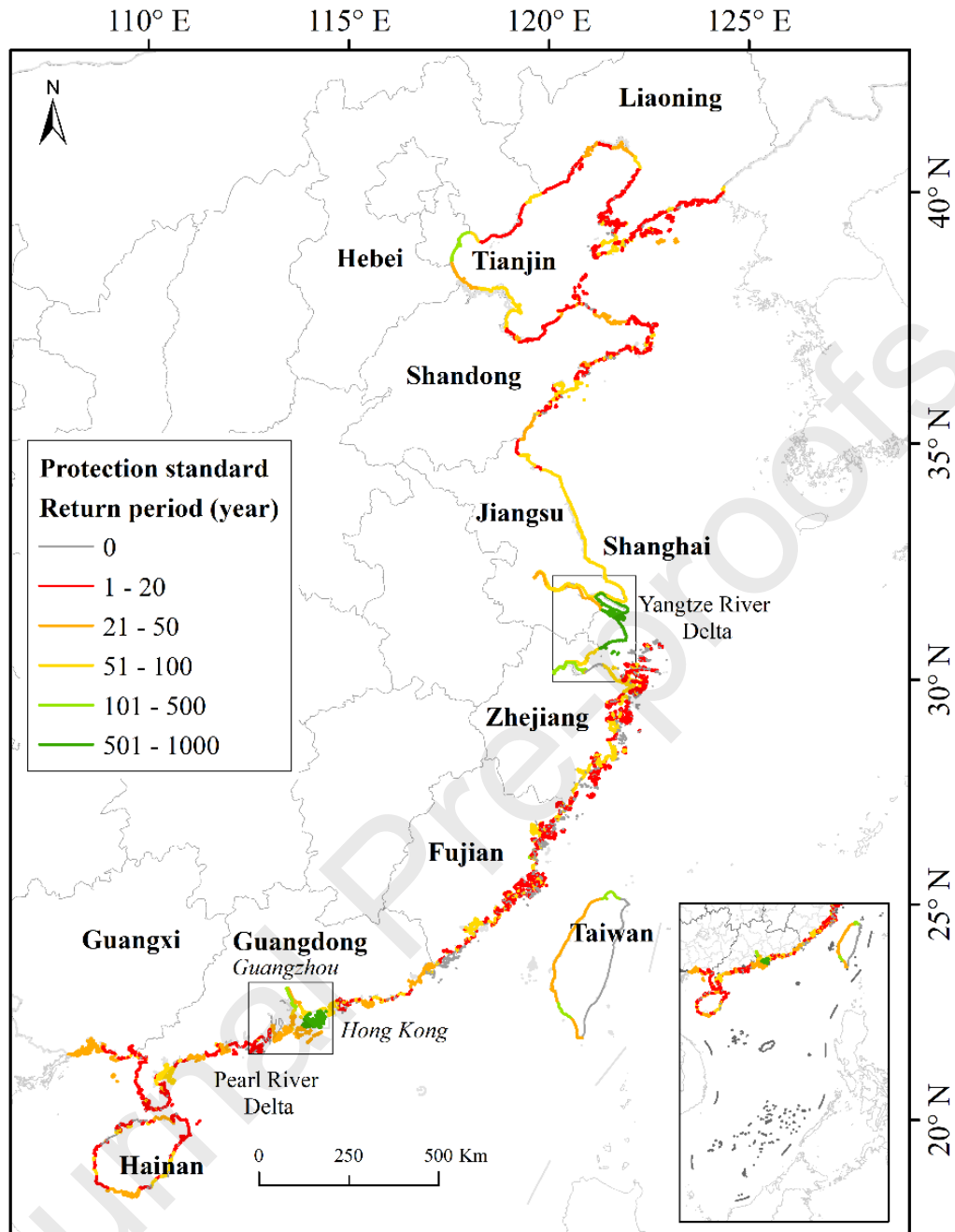
Sandy coast constitutes about 2,703 km, or 9.3% of the country's coastline. It is mainly located in Hainan province with a length of 564 km or 34.0% of the province's coastline. Muddy coast accounts for 6.0% of the national coastline. The length of muddy coast identified in this study is significantly less than previous studies (Wang and Aubrey, 1987). The main reason is that muddy coasts have abundant resources, which are conducive to the development of aquaculture and reclamation for other industries. Given this and its high erosion potential, it has been protected and/or has been converted to artificial coast (Sun et al., 2015; Luo et al., 2015). The length of river mouths is about 137 km, which is consistent with the length of the estuaries and coasts obtained from other studies (e.g. Gao et al., 2013).

1 Tab. 2 Coastline, artificial coastline, areas and population in the low elevation coastal zone (LECZ) areas ($DEM \leq 10$ m) in the first-level administrative
 2 divisions of China.

Province	Coastline (km)	Percent of national coast (%)	Artificial coastline (km)	Percentage of artificial coast to provincial coasts (%)	Territory (km ²)	Areas of LECZ (km ²) AW3D30	LECZ to territory (%)	Total provincial population (million)	Population in LECZ (million) LandScan	Population in LECZ to total province (%)	Population density in LECZ (people/km ²)
Liaoning	2620	9.1	1685	64.3	135,916	12,262	9.0	44.7	6.2	13.8	503
Hebei	376	1.3	307	81.6	176,101	17,663	10.0	71.5	7.8	10.9	442
Tianjin	125	0.4	123	98.7	10,985	9,866	89.8	10.6	9.4	88.6	949
Shandong	2838	9.8	1735	61.1	148,269	21,031	14.2	96.1	8.6	8.9	407
Jiangsu	1247	4.3	1177	94.4	99,227	66,532	67.1	78.1	51.5	65.9	774
Shanghai	635	2.2	631	99.4	6,811	6,458	94.8	17.7	14.7	83.4	2279
Zhejiang	6135	21.2	2287	37.3	103,621	16,005	15.4	49.0	21.9	44.7	1367
Fujian	5042	17.4	1923	38.1	127,161	3,540	2.8	36.4	6.8	18.7	1921
Guangdong	5344	18.5	2758	51.6	191,334	20,243	10.6	91.3	33.3	36.5	1646
Guangxi	1299	4.5	890	68.5	252,891	1,623	0.6	46.9	0.9	1.8	524
Hainan	1647	5.7	190	11.5	38,762	2,554	6.6	8.1	1.9	23.4	736
Hong Kong	653	2.3	483	74.0	1,229	186	15.1	7.0	1.4	19.7	7377
Macau	59	0.2	52	87.9	37	12	32.7	0.4	0.2	38.1	13291
Taiwan	947	3.3	586	61.9	103,621	2,942	2.8	23.0	4.6	20.1	1570
Total	28967	100	14828	51.2	1,395,966	180,916	13.0	580.8	169.2	29.1	934

3 Artificial coastline amounts to 14,828 km in China, which is more than half of the country's
4 coastline (Tab. 2). The artificial coastlines in Tianjin, Jiangsu and Shanghai amount to more
5 than 94% of the provincial coast. The lowest percentage of artificial coastline is Hainan
6 Province covering only 11.5% its coasts. The utilization of the mainland coast in China has
7 increased continuously and dramatically from the 1940s to today, driving the creation of
8 artificial coasts (Wu et al., 2014; Wang et al., 2014). The main reasons for the high
9 percentage of artificial coastlines in China are due to (1) massive land reclamation for the
10 need of land supply (Hou et al., 2016), (2) construction of seawalls and embankments to
11 protect erosion and flooding (Luo et al., 2015), (3) seaward artificial aquaculture which
12 encloses many coastal areas, and (4) seaward artificial wetlands with dikes (Sun et al., 2015)
13 (Supplementary Fig. S3). Extensive land reclamation has occurred in coastal China
14 comprising 13,380 km² from 1950 to 2008 (Fu et al., 2010), especially in Tianjin, Hebei,
15 Jiangsu and Shanghai. The decline of natural coasts and the high percentage of artificial
16 coasts is similar to other studies (e.g. Gao et al., 2013; Hou et al., 2016).

17 After the segmentation, coastal protection standards along coastal China were extracted from
18 Li et al. (2003), Aerts et al. (2009) and Hallegatte et al. (2013) (Fig. 4). Shanghai and Hong
19 Kong have the highest protection level at 1000-year and 900-year return period, respectively.
20 Tianjin and Taipei have 200-year return period. Coastal provincial capitals, such as
21 Hangzhou (200-year) and Guangzhou (200-year), have higher protection standard than other
22 coastal cities, such as Ningbo (100-year), Quanzhou (100-year) and Shenzhen (100-year) .



23

24 Fig. 4 Coastal protection standard (return period) of China.

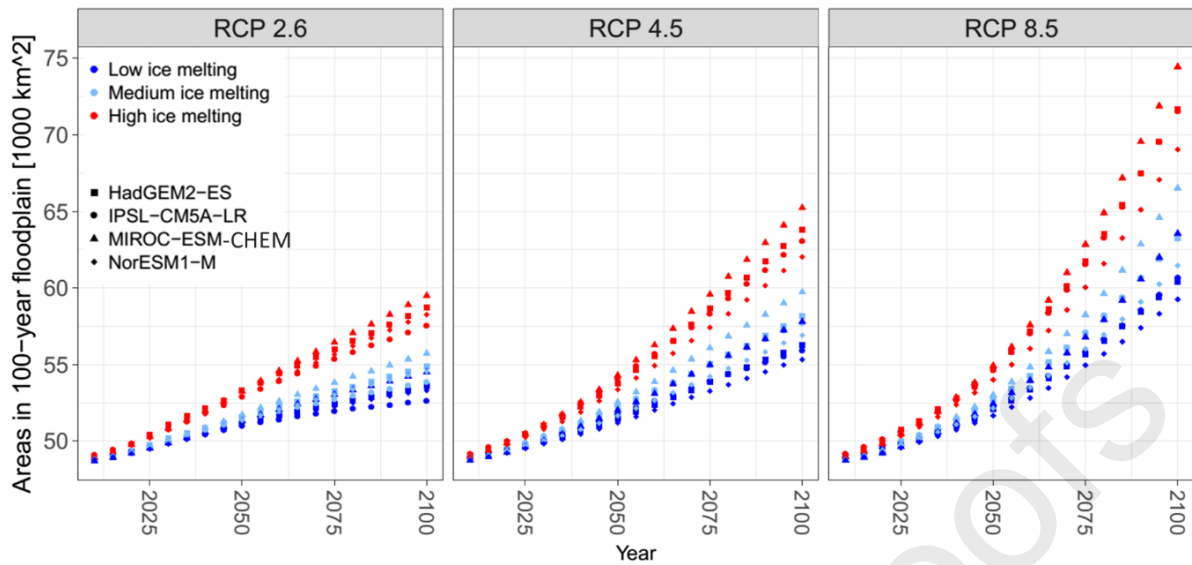
25 According to the DIVA-China database, the total area of the low elevation coastal zone
 26 (LECZ, defined as the contiguous area along the coast that is less than 10 m above the sea
 27 level) in China is 180,916 km², which account for 13.0 % of coastal provincial territory (Tab.
 28 2). Jiangsu Province has the largest LECZ of 66,532 km², which accounts for 67.1 % of its
 29 territory and more than one third of all LECZ in China (Supplementary Fig. S4). Shanghai

30 and Tianjin, two of the largest and most important ports in China, have the largest percentage
31 of LECZ to its territory, at about 95 % and 90 %, respectively. The region with the lowest
32 percentage of LECZ is Guangxi, with only 0.6 %.

33 The LECZ population is ~170 million. Similarly to the LECZ, Jiangsu Province has the
34 largest LECZ population at 51.5 million, or nearly one third of the LECZ population in China
35 (Supplementary Fig. S4), followed by Guangdong Province with 33.3 million. Both Tianjin
36 and Shanghai have the highest percentage of population living in the LECZ, with 88.6 % and
37 83.4 %, respectively. Except for Macau, Guangxi has lowest population of 0.9 million living
38 in LECZ, only accounting for 1.8 % of the total provincial population. Hong Kong and
39 Macau have the highest LECZ population density in China. In Mainland China, Shanghai has
40 the highest LECZ population density with 2,279 people per km². These findings are in the
41 same range as the findings of McGranahan et al. (2007), Neumann et al. (2015) and Liu et al.
42 (2015).

43 **3.2 Exposure of the 100-year return period flood event**

44 Using the high-resolution segmentation, we calculated exposed areas, population and assets
45 (ignoring dikes) in the 100-year coastal floodplain (Fig 5). With SLR, areas below the 100-
46 year floodplain rapidly increase. The 100-year floodplain area is approximately 49,000 km²
47 (2020), growing to 53,000 (RCP2.6) to 74,000 km² (RCP8.5) by 2100. The SLR scenario of
48 RCP8.5 under the MIROC-ESM-CHEN model, combined with high ice melting scenario, is
49 the scenario with the highest relative sea level rise and the largest floodplain under all GCM-
50 RCP-ice melting combinations. RCP2.6 under the NorESM1-M model, combined with a low
51 ice melting scenario, is the lowest SLR scenario and the smallest flooded area. In this study,
52 the area of the 100-year floodplain depends only on the SLR scenario, as we assume,
53 following 20th century observations (Menendez and Woodworth, 2011), extreme water levels
54 to increase uniformly with sea-level rise.



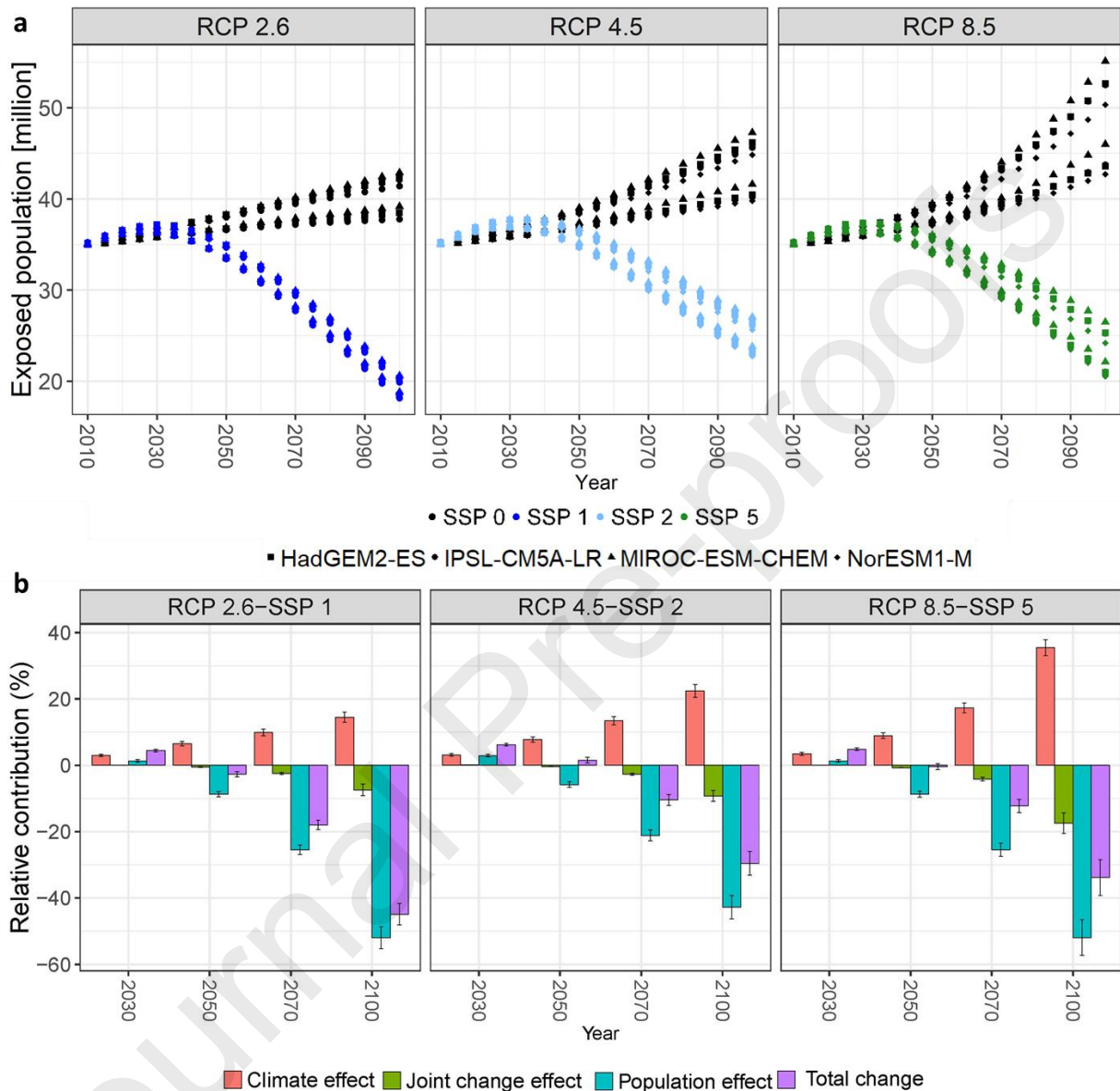
55

56 Fig. 5 Areas of the 100-year coastal floodplain over the 21st century under SLR scenarios.

57

58 The exposed population in SSP0 is lower compared with the other four SSPs before 2030
 59 because of the assumption of no growth of population. After 2030, the exposed population
 60 keeps increasing under SSP0, while they decrease under the other four SSPs due to the
 61 decline of total population in these scenarios (Fig. 6a). Considering demographic changes and
 62 SLR, the 100-year floodplain exposed population is 36.5 million (2020) people, changing to
 63 18.1-27.0 million (2100). Under RCP2.6-SSP1, RCP4.5-SSP2 and RCP8.5-SSP5, the
 64 exposed population shows a decreasing trend after peaking around 2030 with the greatest
 65 decline in RCP2.6-SSP1. To analyse the temporal change in exposure and relative
 66 contribution due to climate, population and joint change effects, we calculate the annual
 67 relative contribution (Fig. 6b) as a percentage change, as defined in Eq.2. The sum of these is
 68 known as the total change. Sea-level rise (climate effect) always leads to increasing
 69 population exposure in the 21st century. Before 2030, exposed population is still increasing.
 70 The population change leads to increased exposure at the beginning of this century but then
 71 leads to a reduction after 2040. The population effect becomes more prominent than

72 population and joint change effects, which leads to the total decrease of exposed population.
 73 Thus, change in population exposure to coastal floods is mainly due to the population effect.



74
 75 Fig. 6 a) Population below 100-year coastal floodplain under RCP-SSP scenarios in the 21st
 76 century; b) Relative contribution of changes to exposed population (below 100-year coastal
 77 floodplain) under SSP-RCP scenarios. Error bars illustrate the standard deviation in total
 78 exposure change across scenarios for each effect.

79

80 Considering demographic changes, the assets below 100-year floodplain are US\$ 1.6 trillion
 81 (2020), which grows to US\$ 4.5-11.1 trillion (2100). Exposed assets increases before 2050 in
 82 RCP2.6-SSP1, then begin to decline slightly. Except for the RCP2.6-SSP1, the effected assets

83 under the other three combination shows upward trends, with RCP8.5-SSP5 showing the
 84 highest increase.

85 3.3 Risks and adaptation costs

86 The expected number of people flooded annually is presented in Fig. 7a. Due to protection,
 87 the population flooded is much smaller than the exposed population. The expected number of
 88 people flooded annually is highest under RCP8.5-SSP5 and lowest in RCP2.6-SSP1. Flooded
 89 population grows slightly slower at the beginning of the century, increase slowly until 2050
 90 (less than 0.25 m relative SLR), then accelerates faster, especially after 2070.

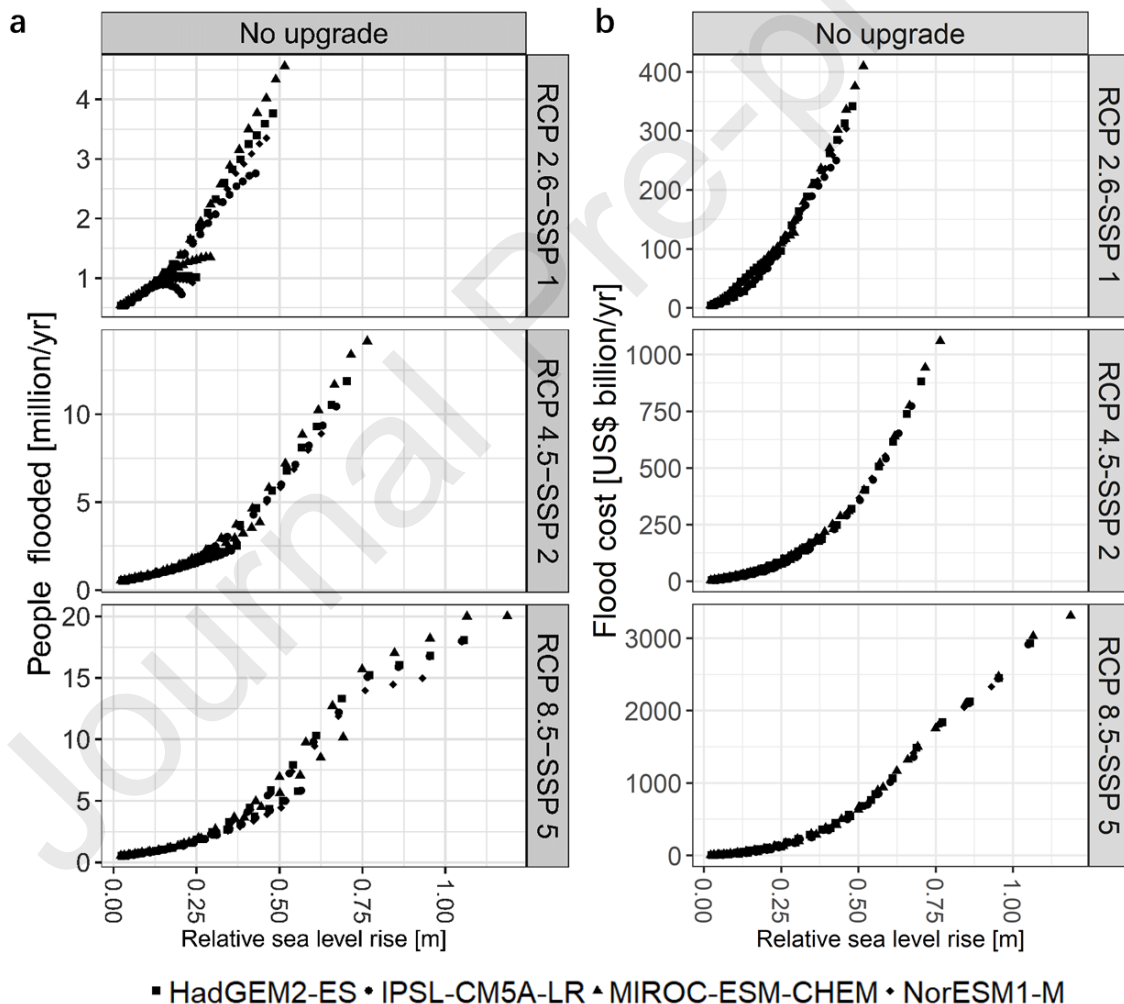
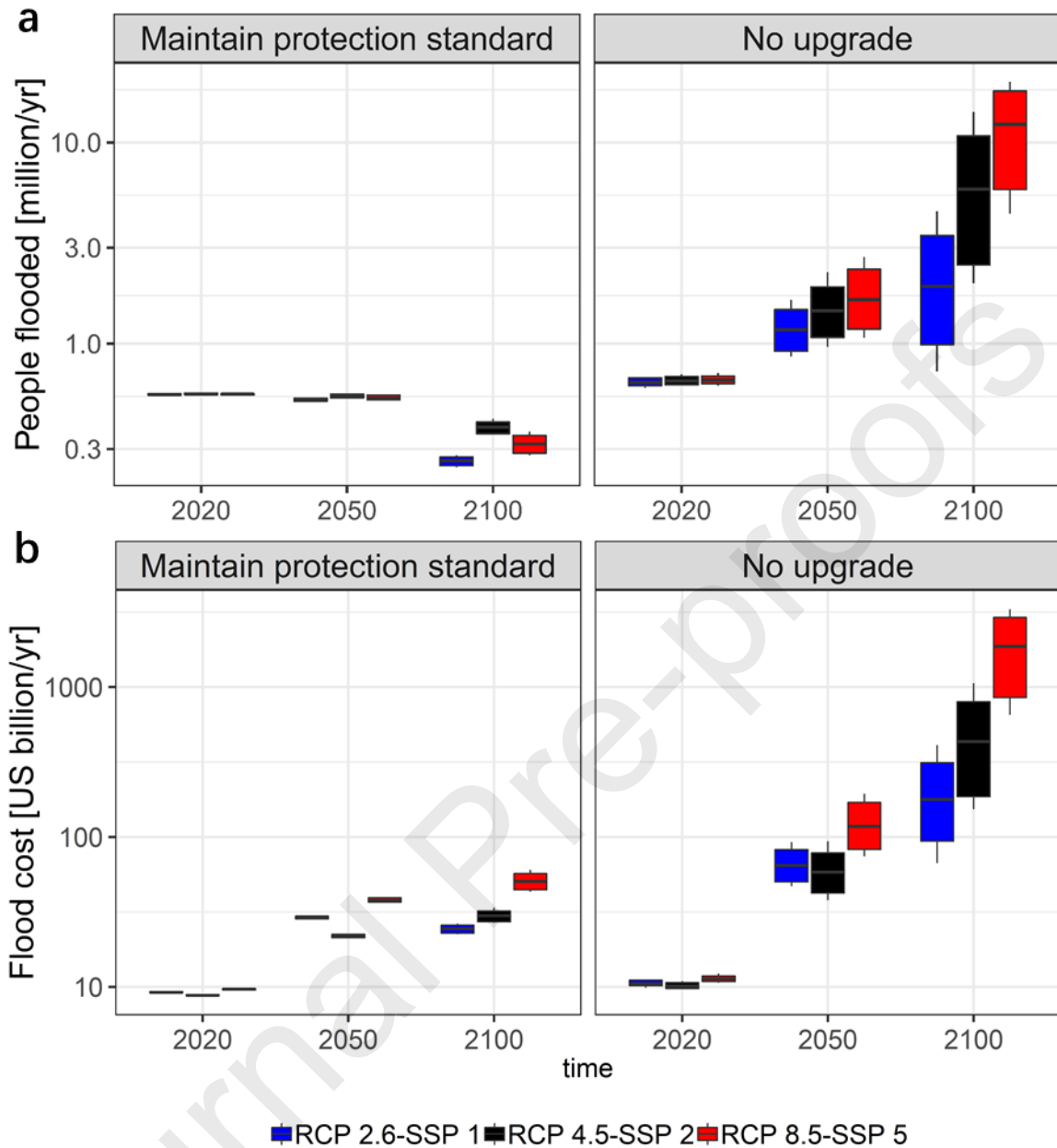


Fig. 7 People flooded and flood cost of China with relative sea level rise in the 21st century under a no upgrade to adaptation strategy with respect to 2010.

95 The number of people flooded per year is about 0.6 million in 2020, increasing to ~0.7 to 20
96 million people per year at end of this century if there is no upgrading to protection levels.
97 This number drops to 0.2 to 0.4 million with maintaining protection standard (Fig. 8). The
98 change of population flooded shows that the effect of adaptation strategy and declines of total
99 population exceeds the climate effect under the maintaining the constant protection. The lack
100 of update in protection and the climate effect lead to higher population exposure, even when
101 there are declines of total population. Hence, maintaining constant protection reduces impacts
102 by about one order of magnitude.

103 The flood costs are shown in Fig.7b. Flood costs are highest under RCP8.5-SSP5 and the
104 lowest under RCP2.6-SSP1. Flood costs grow slower at the beginning of the century, but then
105 accelerates faster reflecting an accelerating rise in sea-level. The average annual flood cost is
106 about US\$ 10 billion per year in 2020. This increases by ~7–330 times to US\$ 67-3,308
107 billion per year by the end of 21st century under the most pessimistic scenario, with no
108 upgrade. This number drops to US\$ 22-60 billion flood damage per year with maintaining
109 constant protection standards (Fig. 8).



110

111 Fig. 8 People flooded and flood costs in 2020, 2050 and 2100 under two adaptation strategies.
 112 On each box, the central mark indicates the median, and the bottom and top edges of the box
 113 indicate the 25th and 75th percentiles, respectively. The whiskers extend to the most extreme
 114 (maximum and minimum) data points.

115

116 We investigated dike costs under two adaptation strategies. If there is no upgrade of
 117 protection and the dike that was built in 2010 with costs of US\$ 644 billion, then there are no
 118 additional capital costs for building and upgrading dikes but only costs for maintenance of
 119 existing dikes. With rise of sea-level, parts of dikes are no longer effective, thus dike costs

120 decrease with SLR under no upgrade. Under maintaining protection standards, dikes remain
 121 effective, dike costs range from US\$ 8-10 billion per year under RCP2.6-SSP1 to US\$ 11-17
 122 billion under RCP8.5-SSP5 in 2100 (Tab. 3). Comparing flood costs and dike costs, increased
 123 dike costs are two orders of magnitude smaller than reduced flood costs across all scenarios,
 124 even without accounting for indirect damages.

125 Tab. 3 Dike and flood costs in 2100 under multiple scenarios. The median and, in parentheses, the
 126 maximum and minimum values are provided. In the last two columns, the median value is
 127 considered to calculate reduced flood costs and increased dike costs.

RCP-SSP	Flood costs (US\$billion/yr)		Dike costs (US\$billion/yr)		Reduced flood costs	Increased dike costs
	No upgrade	Maintain protection standard	No upgrade	Maintain protection standard		
RCP2.6-SSP1	210 (67, 410)	24 (22, 26)	6 (4, 7)	9 (8, 10)	186 (45, 383)	3 (1, 6)
RCP4.5-SSP2	521 (153, 1060)	30 (28, 34)	4 (2, 6)	10 (9, 12)	491 (126, 1026)	6 (3, 10)
RCP8.5-SSP5	1916 (650, 3308)	51 (43, 60)	2 (0.1, 5)	14 (11, 17)	1865 (607, 3248)	12 (6, 17)

128

129

130 3.4 Implications

131 This study quantitatively assesses people effect by sea-level rise, plus flood damage and
 132 adaptation costs for coastal China using the DIVA modelling framework and considering
 133 three RCP and SSP combinations and two adaptation strategies. The results show that coastal
 134 flood risk highly depends on change in population and coastal adaptation. Sustainable
 135 development (RCP2.6-SSP1) would at least halve the damages or reduce by one order of
 136 magnitude the flood costs compared to a moderate development (RCP4.5-SSP2) or a fossil-
 137 fuel based development scenario (RCP8.5-SSP5). The intensification of ESLs with global
 138 warming is the main contributor of the increasing coastal flood risk in China. From a strategic
 139 planning perspective, coastal hard engineering protection is very effective in protecting coasts.

140 The expense of protection (dike costs) is much smaller than reduced flood damage, not to
141 mention indirect damages (e.g. damages caused by failure of coastal infrastructure network)
142 which have not been assessed here. The methods and findings can be used to provide basic
143 information to governments, policy-makers, insurance companies and local communities on
144 the overall risk at a national scale and pinpoint hotspots within coastal China for further more
145 detailed analysis.

146 Few studies have assessed the potential costs of adaptation to coastal flood risks in China, yet
147 such estimates and subsequent actions remain a huge challenge due to the uncertainties of
148 future ESLs, variation of adaptation strategies, and socio-economic settings. Many other
149 drivers influence impacts that cannot be fully accounted in models due to the quality and the
150 lack of available datasets and constraints of computer simulation of coastal behaviours at a
151 large scale. Additionally, the datasets may not address recent policy advancements. For
152 instance, China has scrapped the one-child policy, which has not been considered in SSPs
153 (Jiang et al., 2017), which will probably increase the population exposure to flooding. We
154 also assume homogeneous population change in national scale, without considering
155 urbanisation, urbans sprawl and coastal mitigation (Merkenes et al., 2018). Considering
156 domestic migration and urbanisation, coastal China attracts more population than inland areas,
157 leading to a higher population exposed to coastal flooding. Second, during the segmentation,
158 we visually interpreted remote sensing images, which encompasses to a certain degree of
159 subjectivity. This could be improved by working with local authorities and carrying out field
160 investigations to validate this dataset. Meanwhile, China's coast is highly dynamic due to
161 intensive human and economic activities (e.g coastal reclamation), which the current
162 simulation is not able to model. Segmentation and reclassification may usefully be repeated
163 in five or ten years' time, drawing on automated methods that are presently being derived
164 (Luijendijk et al., 2018). Evidence indicates that fatalities from storm surges are decreasing in

165 China as communities are becoming more resilient against coastal flooding by strengthening
166 institutional arrangements, adaptation and mitigation actions (Fang et al., 2017). Hence,
167 future flood risk could be lower than estimates presented here. Moreover, we used simplified
168 assumptions, such as stationary storm systems, and linear superposition of relative sea level
169 rise and surge. Cyclones are for instance, underrepresented in the GTSR dataset used (Muis et
170 al., 2016). Additionally, waves are not considered due to data availability. Cyclones may
171 intensify with climate change, thus further rising extreme sea levels (including surge and
172 waves) during storm conditions (Wahl et al., 2017; Vousdoukas et al., 2018). The
173 contribution of SLR to coastal flood risk will probably increase beyond 2100 considering the
174 lagged effects of the deep ocean and contribution of Antarctic ice sheet (Deconto and Pollard,
175 2016) meaning long-term adaptation is essential. Coastal flooding may be compounded by
176 other sources such as extreme precipitation and river discharge, leading to worse impacts
177 (Wahl et al., 2015). Lastly, human-induced subsidence due to ground fluid depletion has not
178 been included due to lack of consistent data, even though it is widely observed and has
179 caused large damages along coastal China (Xue et al., 2005), especially in the large cities (e.g.
180 Shanghai and Tianjin). Subsidence will exacerbate the impacts of SLR and requires further
181 investigations in a Chinese context.

182 Presently, hard engineering of building and enhancing dikes and seawalls are still the main
183 form of adaptation measure. Hardening coasts threatens coastal biodiversity and ecosystems
184 (Ma et al., 2014). Simultaneously, soft engineering approaches, which put more emphasis on
185 the natural environment, such as mangrove afforestation, wetland creation, and/or combined
186 engineering structures, such as seawall with wetland creation/beach nourishment, have
187 become increasingly popular in recent years (Luo et al., 2015). To protect coastlines against
188 extreme conditions coastal communities could reinforce current adaptation approaches,

189 encourage the uptake and harness of new adaptation approaches, such as hybrid adaptation.
190 Thus, a more comprehensive analyses of coastal adaptation options for China is required.

191

192 **4 Conclusion**

193 This study provides a quantitative risk assessment for coastal flood at national level by
194 applying the Dynamic Interactive Vulnerability Assessment (DIVA) model in China. A high-
195 resolution DIVA-China database for coastal China including coastal protection level
196 information has been built to improve the assessment. Compared with the global dataset, it
197 provides a more realistic spatial representation of coastal flood impacts for China, with a 136%
198 increase of coastline length from 12,288 km to 28,966 km. Artificial coasts comprise more
199 than 50% of total coastline length in China, which indicates the necessity of considering
200 protection in the impact assessment.

201 Taking into account data and scenario uncertainties, the 100-year floodplain area covers an
202 extent of 53,000 to 74,000 km² with 18.1-27.0 million exposed population and US\$ 4.5-11.1
203 trillion exposed assets with 21-119 cm of relative SLR in China in 2100. In terms of risk,
204 there are 0.7-20.0 million people expected to be flooded annually in 2100 assuming no
205 upgrade to adaptation, and US\$ 67-3,308 billion assets are at risk per year assuming no
206 upgrade of protection compared with 2100. In contrast, maintaining current protection level,
207 reduce protected impacts to 0.2-0.4 million people/yr and US\$ 22-60 billion/yr flood costs by
208 2100, at only US\$ 8-17 billion/yr of dike costs. Increased dike costs are two orders of
209 magnitude smaller than reduced flood costs across all scenarios, even without accounting for
210 indirect damages.

211 This research will be helpful to governments, policy-makers, insurance companies and local
212 communities in China to provide information for designing strategies to adapt to increasing

213 coastal flood risk. In particular, it can be updated and improved if there are better quality
 214 regional datasets available and modification of model algorithms/assumptions, to provide
 215 consistent, comparable and rapid coastal flood risk assessments for stakeholder needs.

216 **Acknowledgements**

217 This work is funded by the National Key R & D Program of China (2017YFE0100700;
 218 2016YFA0602404; 2017YFC1503001); Shanghai Sailing Program (19YF1413700); China
 219 Postdoctoral Science Foundation (No. 2019M651429); European Union's Seventh
 220 Programme for Research, Technological Development and Demonstration under grant
 221 agreement No. 603396 (RISES-AM project); Special thanks to China Scholarship Council.

222 **References**

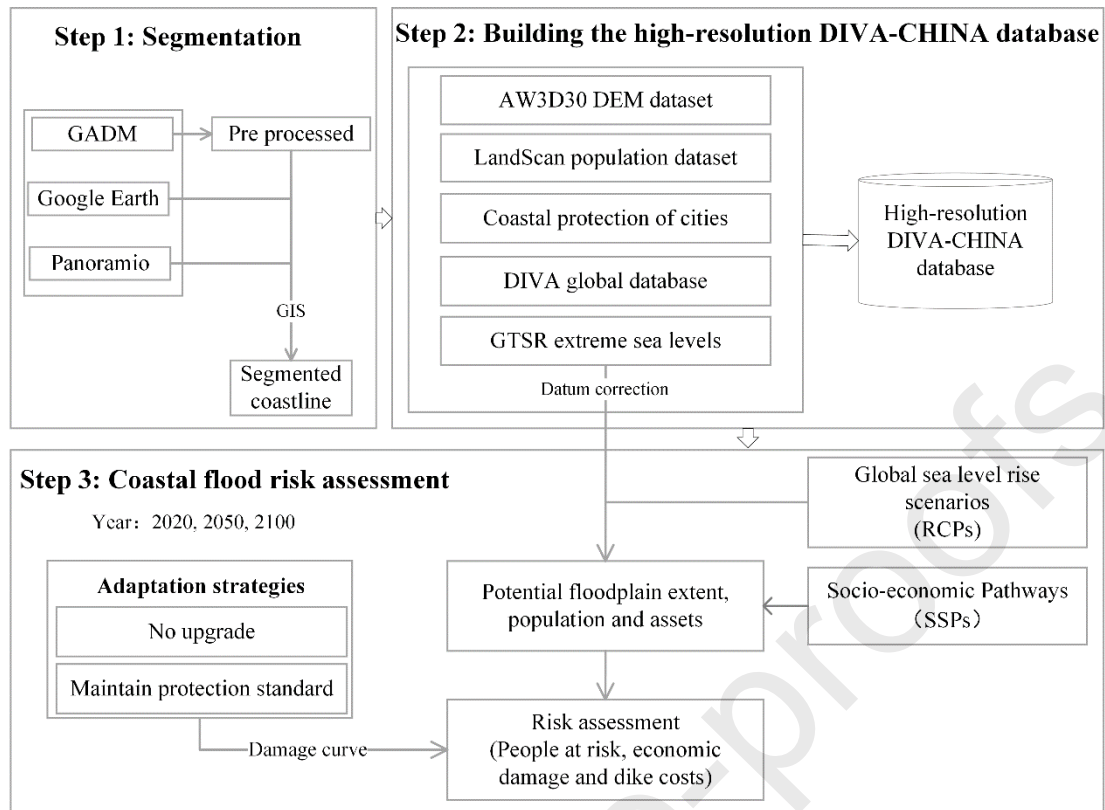
- 223 [1] Aerts, J., Major, D.C., Bowman, M.J., et al. 2009. Connecting delta cities: coastal cities, flood
 224 risk management and adaptation to climate change. VU University Press.
- 225 [2] Bright, E. A., et al. 2011. LandScan 2010. Oak Ridge, TN, Oak Ridge National Laboratory.
- 226 [3] Courtya, L.G., Soriano-Monzalvoa, J.C., and Pedrozo-Acuñaa, A. 2017. Evaluation of open-
 227 access global digital elevation models (AW3D30, SRTM and ASTER) for flood modelling
 228 purposes.
- 229 [4] Fang, J., Liu, W., Yang, S., et al. 2017. Spatial-temporal changes of coastal and marine disasters
 230 risks and impacts in Mainland China. *Ocean Coast. Manag.* 139, 125-140.
- 231 [5] Fu, Y.B., Cao, K., Wang, F., and Zhang, F.S., 2010. Primary quantitative evaluation method on
 232 sea enclosing and land reclamation strength and potential. *Ocean Dev. Manag.* 1, 27-30. (in
 233 Chinese)
- 234 [6] DeConto, R.M., and Pollard, D. 2016. Contribution of Antarctica to past and future sea-level rise.
 235 *Nature* 531(7596):591-597.
- 236 [7] Gao, Y, Wang, H., Su, F., et al. 2013. Spatial and temporal of continental coastline of China in
 237 recent three decades. *Acta Oceanol. Sin.* 35(06), 31-42. (in Chinese)
- 238 [8] Hallegatte, S., Green, C., Nicholls, R.J., et al. 2013. Future flood losses in major coastal cities.
 239 *Nat. Clim. Change* 3(9), 802-806.
- 240 [9] Han, M., Hou, J., and Wu, L. 1995. Potential impacts of sea-level rise on China's coastal
 241 environment and cities: A national assessment. *J. Coastal Res.* 79-95.
- 242 [10] Hanson, S., Nicholls, R.J., Ranger, N., et al. 2011. A global ranking of port cities with high
 243 exposure to climate extremes. *Clim. Change* 104(1), 89-111.
- 244 [11] Hinkel, J. and Klein, R.J., 2009. Integrating knowledge to assess coastal vulnerability to sea-level
 245 rise: The development of the DIVA tool. *Glob. Environ. Change* 19(3), 384-395.
- 246 [12] Hinkel, J., Lincke, D., Vafeidis, A.T., Perrette, M., Nicholls, R.J., Tol, R.S., Marzeion, B.,
 247 Fettweis, X., Ionescu, C. and Levermann, A., 2014. Coastal flood damage and adaptation costs
 248 under 21st century sea-level rise. *Proc. Natl. Acad. Sci. U. S. A.* 111(9), 3292-3297.
- 249 [13] Hou, X., Wu, T., Hou, W., Chen, Q., Wang, Y. and Yu, L. 2016. Characteristics of coastline
 250 changes in mainland China since the early 1940s. *Sci. China: Earth Sci.* 59(9), 1791-1802.
- 251 [14] Hu, P., Zhang, Q., Shi, P., Chen, B. and Fang, J., 2018. Flood-induced mortality across the globe:
 252 Spatiotemporal pattern and influencing factors. *Sci. Total Environ.* 643, pp.171-182.

- 253 [15] Hu, Z., Peng, J., Hou, Y. and Shan, J., 2017. Evaluation of Recently Released Open Global
254 Digital Elevation Models of Hubei, China. *Remote Sens.* 9(3), 262.
- 255 [16] Huang, Q., He, C., Gao, B., et al. 2015. Detecting the 20 year city-size dynamics in China with a
256 rank clock approach and DMSP/OLS nighttime data, *Landsc. Urban Plan.* 137: 138-148.
- 257 [17] Huang, Z., Zong, Y., and Zhang, W. 2004. Coastal inundation due to sea level rise in the Pearl
258 River Delta, China. *Nat. Hazards* 33(2), 247-264.
- 259 [18] International Institute for Applied Systems Analysis. 2012. Shared Socioeconomic Pathways
260 Database. Available at <https://secure.iiasa.ac.at/web-apps/ene/SspDb>.
- 261 [19] Jiang, T., Zhao, J., Jing, C., et al. 2017. National and provincial population projected to 2100
262 under the shared socioeconomic pathways in China. *Adv Climate Change Res.* 13(02), 128-137.
263 (in Chinese)
- 264 [20] Jones, B., O'Neill, B.C., McDaniel, L., McGinnis, S., Mearns, L.O. and Tebaldi, C., 2015. Future
265 population exposure to US heat extremes. *Nat. Clim. Change* 5(7), 652.
- 266 [21] Kang, L., Ma, L., and Liu, Y. 2016. Evaluation of farmland losses from sea level rise and storm
267 surges in the Pearl River Delta region under global climate change. *J. Geogr. Sci.* 26(4), 439-456.
- 268 [22] Ke Q. 2014. Flood risk analysis for metropolitan areas -a case study for Shanghai[D]. TU Delft,
269 Delft University of Technology.
- 270 [23] Kebede, A.S., and Nicholls, R.J. 2012. Exposure and vulnerability to climate extremes:
271 population and asset exposure to coastal flooding in Dar es Salaam, Tanzania. *Reg. Envir. Chang.*
272 12(1), 81-94.
- 273 [24] Leimbach, M., Kriegler, E., Roming, N., and Schwanitz, J. 2017. Future growth patterns of world
274 regions – A GDP scenario approach. *Glob. Environ. Change.* 42, 215–225.
- 275 [25] Li, W., Wang, J., and Chen, L. 2003. Study on storm surge protection standard of seawall
276 engineering. *Water Resource Planning. Des* 4:5–9. (in Chinese)
- 277 [26] Li, X., Rowley, R. J., and Kostelnick, J. C. 2009. GIS Analysis of Global Impacts from Sea Level
278 Rise. *Photogramm. Eng. Remote Sens.* 75(7), 807-818.
- 279 [27] Liao, X., Xu, W., Zhang, J., Li, Y. and Tian, Y., 2019. Global exposure to rainstorms and the
280 contribution rates of climate change and population change. *Sci. Total Environ.* 663, pp.644-653.
- 281 [28] Liu, C. 2014. Reflections on Maritime Partnership: Building the 21st Century Maritime Silk
282 Road. China Institute of International Studies.
- 283 [29] Liu, J., Wen, J., Huang, Y., et al. 2015. Human settlement and regional development in the
284 context of climate change: a spatial analysis of low elevation coastal zones in China. *Mitig.*
285 *Adapt. Strateg. Glob. Chang.* 20(4), 527-546.
- 286 [30] Luijendijk, A., Hagenaaars, G., Ranasinghe, R., Baart, F., Donchyts, G. and Aarninkhof, S., 2018.
287 The state of the world's beaches. *Sci. Rep.* 8(1), 6641.
- 288 [31] Luo, S., Cai, F., Liu, H., et al. 2015. Adaptive measures adopted for risk reduction of coastal
289 erosion in the People's Republic of China. *Ocean Coast. Manag.* 103, 134-145.
- 290 [32] Ma, Z., Melville, D.S., Liu, J., et al. 2014. Rethinking China's new great wall. *Science* 346(6212),
291 912-914.
- 292 [33] McFadden, L., Nicholls, R.J., Vafeidis, A. and Tol, R.S., 2007. A methodology for modeling
293 coastal space for global assessment. *J. Coast. Res.* 911-920.
- 294 [34] McGranahan, G., Balk, D., and Anderson, B. 2007. The rising tide: assessing the risks of climate
295 change and human settlements in low elevation coastal zones. *Environ. Urban.* 19(1), 17-37.
- 296 [35] Menéndez, M. and Woodworth, P.L., 2010. Changes in extreme high water levels based on a
297 quasi - global tide - gauge data set. *J. Geophys. Res.: Oceans* 115(C10).
- 298 [36] Merkens, J-L., Lincke, D., Hinkel, J., Brown, S., Vafeidis, A.T. 2018. Regionalisation of
299 population growth projections in coastal exposure analysis. *Clim. Change* 14(1):3.
- 300 [37] Messner F, et al. 2007. Evaluating flood damages: Guidance and recommendations on principles
301 and methods FLOOD-site Project Deliverable D9.1. Available at
302 [http://www.floodsite.net/html/partner_area/project_docs/T09_06_01_Flood_damage_guidelines_](http://www.floodsite.net/html/partner_area/project_docs/T09_06_01_Flood_damage_guidelines_d9_1_v2_2_p44.pdf)
303 [d9_1_v2_2_p44.pdf](http://www.floodsite.net/html/partner_area/project_docs/T09_06_01_Flood_damage_guidelines_d9_1_v2_2_p44.pdf). Accessed August 26, 2019.
- 304 [38] Muis, S., Verlaan, M., Winsemius, H.C., Aerts, J.C. and Ward, P.J., 2016. A global reanalysis of
305 storm surges and extreme sea levels. *Nat. Commun.* 7.

- 306 [39] Nicholls, R.J. 2004. Coastal flooding and wetland loss in the 21st century: changes under the
 307 SRES climate and socio-economic scenarios. *Glob. Environ. Change* 14(1), 69-86.
- 308 [40] Nicholls, R.J., Wong, P.P., Burkett, V., Woodroffe, C. D., and Hay, J. 2008. Climate change and
 309 coastal vulnerability assessment: scenarios for integrated assessment. *Sustain. Sci.* 3(1), 89-102.
- 310 [41] Nicholls, R.J., Hanson, S.E., Lowe, J.A., Warrick, R.A., Lu, X. and Long, A.J., 2014. Sea-level
 311 scenarios for evaluating coastal impacts. *Wiley Interdiscip. Rev.-Clim. Chang.* 5(1), 129-150.
- 312 [42] Neumann, B., Vafeidis, A. T., Zimmermann, J., and Nicholls, R.J. 2015. Future coastal
 313 population growth and exposure to sea-level rise and coastal flooding - a global assessment. *Plos*
 314 *One*, 10(3), e0131375.
- 315 [43] O'Neill, B.C., Kriegler, E., Riahi, K., et al. 2014. A new scenario framework for climate change
 316 research: the concept of shared socioeconomic pathways. *Clim. Change* 122(3), 387-400.
- 317 [44] Peltier, W.R., 2000. Glacial isostatic adjustment corrections. In: Douglas, B.C; Kearney, M.S.,
 318 and Leatherman, S.P. (eds.), *Sea level rise: History and consequences*. San Diego, California:
 319 Academic Press, 65-95.
- 320 [45] Samir, K.C. and Lutz, W., 2014. Demographic scenarios by age, sex and education
 321 corresponding to the SSP narratives. *Popul. Env.* 35(3), pp.243-260.
- 322 [46] Samir, K.C. and Lutz, W., 2017. The human core of the shared socioeconomic pathways:
 323 Population scenarios by age, sex and level of education for all countries to 2100. *Glob. Environ.*
 324 *Change* 42, 181-192.
- 325 [47] Seto, K.C. 2011. Exploring the dynamics of migration to mega-delta cities in Asia and Africa:
 326 Contemporary drivers and future scenarios. *Glob. Environ. Change* 21, S94-S107.
- 327 [48] Standard for Flood Control. (National Standard of the People's Republic of China.GB 50201-
 328 2014) [S]. 2014. Ministry of Housing and Urban-Rural Development of the People's Republic of
 329 China.
- 330 [49] Sun, Z., Sun, W., Tong, C., Zeng, C., Yu, X. and Mou, X., 2015. China's coastal wetlands:
 331 Conservation history, implementation efforts, existing issues and strategies for future
 332 improvement. *Environ. Int.* 79, 5-41.
- 333 [50] T. Tadono, H. Nagai, H. Ishida, F. Oda, S. Naito, K. Minakawa, H. Iwamoto. 2016.1 Validation
 334 of the 30 m-mesh Global Digital Surface Model Generated by ALOS PRISM, The International
 335 Archives of the Photogrammetry, Remote Sensing and Spatial Information Sciences, ISPRS, Vol.
 336 XLI-B4, pp.157-162.
- 337 [51] Vafeidis, A.T., Nicholls, R.J., McFadden, L., Tol, R.S., Hinkel, J., Spencer, T., Grashoff, P.S.,
 338 Boot, G. and Klein, R.J., 2008. A new global coastal database for impact and vulnerability
 339 analysis to sea-level rise. *J. Coastal Res.* 917-924.
- 340 [52] Van Vuuren D.P., Carter T.R. 2014. Climate and socio-economic scenarios for climate change
 341 research and assessment: reconciling the new with the old. *Clim. Change* 122(3): 415-429.
- 342 [53] van Vuuren DP, Edmonds J, Kainuma M, Riahi K, Thomson A, Hibbard K, Hurtt GC, Kram T,
 343 Krey V, Lamarque J-F, Masui T, Meinshausen M, Nakicenovic N, Smith SJ, Rose SK. 2011. The
 344 representative concentration pathways: An overview. *Clim. Change*, 109(1-2), 5–31.
- 345 [54] Voudoukas, M.I., Mentaschi, L., Voukouvalas, E., Bianchi, A., Dottori, F. and Feyen, L., 2018.
 346 Climatic and socioeconomic controls of future coastal flood risk in Europe. *Nat. Clim. Change*
 347 8(9), p.776.
- 348 [55] Wahl, T., Haigh, I.D., Nicholls, R.J., et al. 2017. Understanding extreme sea levels for broad-
 349 scale coastal impact and adaptation analysis. *Nat. Commun.* 8: 16075.
- 350 [56] Wahl, T., Jain, S., Bender, J., et al. 2015. Increasing risk of compound flooding from storm surge
 351 and rainfall for major US cities. *Nat. Clim. Change* 5(12), 1093-1097.
- 352 [57] Wang, J., Yi, S., Li, M.Y., Wang, L., and Song, C. 2018. Effects of sea level rise, land
 353 subsidence, bathymetric change and typhoon tracks on storm flooding in the coastal areas of
 354 Shanghai. *Sci. Total Environ.* 621:228-234.
- 355 [58] Wang B, Chen S, Zhang K, et al. 1995. Potential impacts of sea-level rise on the Shanghai area. *J.*
 356 *Coastal Res.* 151-166.
- 357 [59] Wang W, Liu H, Li Y, et al. 2014. Development and management of land reclamation in China.
 358 *Ocean Coast. Manag.* 102: 415-425.

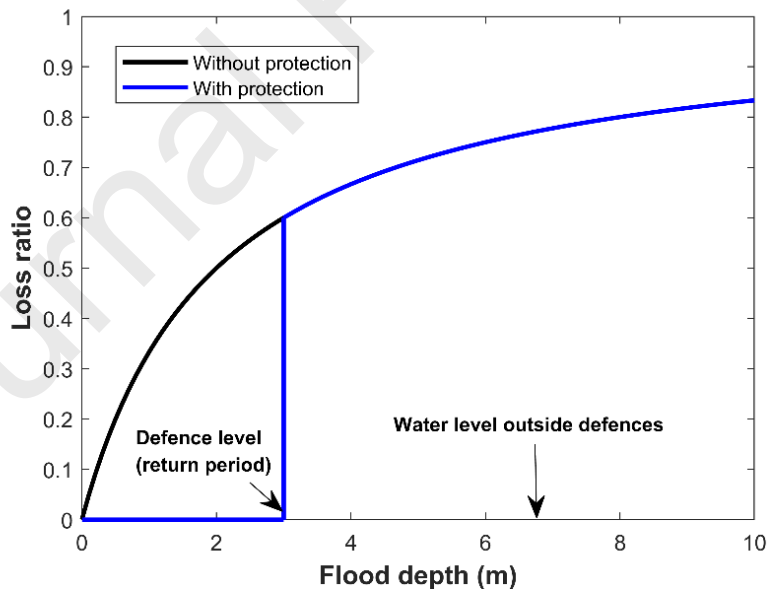
- 359 [60] Wang, Y. and Aubrey, D.G., 1987. The characteristics of the China coastline. *Cont. Shelf Res.*
360 7(4), 329-349.
- 361 [61] Wang, Y., 1980. The coast of China. *Geoscience Canada*, 7(3).
- 362 [62] Wolff, C., Vafeidis, A.T., Lincke, D., Marasmi, C. and Hinkel, J., 2016. Effects of Scale and
363 Input Data on Assessing the Future Impacts of Coastal Flooding: An Application of DIVA for
364 the Emilia-Romagna Coast. *Front. Mar. Sci.* 3, 41.
- 365 [63] Wolff, C., Vafeidis, A.T., Muis, S., et al. 2018. A Mediterranean coastal database for assessing
366 the impacts of sea-level rise and associated hazards. *Sci. Data* 5, 180044.
- 367 [64] Wu, J., Li, N., and Shi, P. 2014. Benchmark wealth capital stock estimations across China's 344
368 prefectures: 1978 to 2012. *China Econ. Rev.* 31: 288-302.
- 369 [65] Wu, T., Hou, X. and Xu, X., 2014. Spatio-temporal characteristics of the mainland coastline
370 utilization degree over the last 70 years in China. *Ocean Coast. Manag.* 98, 150-157.
- 371 [66] Xu, M., He, C., Liu, Z. and Dou, Y., 2016. How did urban land expand in China between 1992
372 and 2015? A multi-scale landscape analysis. *PloS one*, 11(5), p.e0154839.
- 373 [67] Xue, Y.Q., Zhang, Y., Ye, S.J., et al. 2005. Land subsidence in China. *Environmental geology.*
374 48(6), 713-720.
- 375 [68] Yin, J., Yin, Z., Yu, D.P. and Xu, S.Y. 2012. Vulnerability analysis for storm induced flood: a
376 case study of Huangpu River Basin. *Scientia Geographica Sinica.* 32(9), 1155-1160.

377



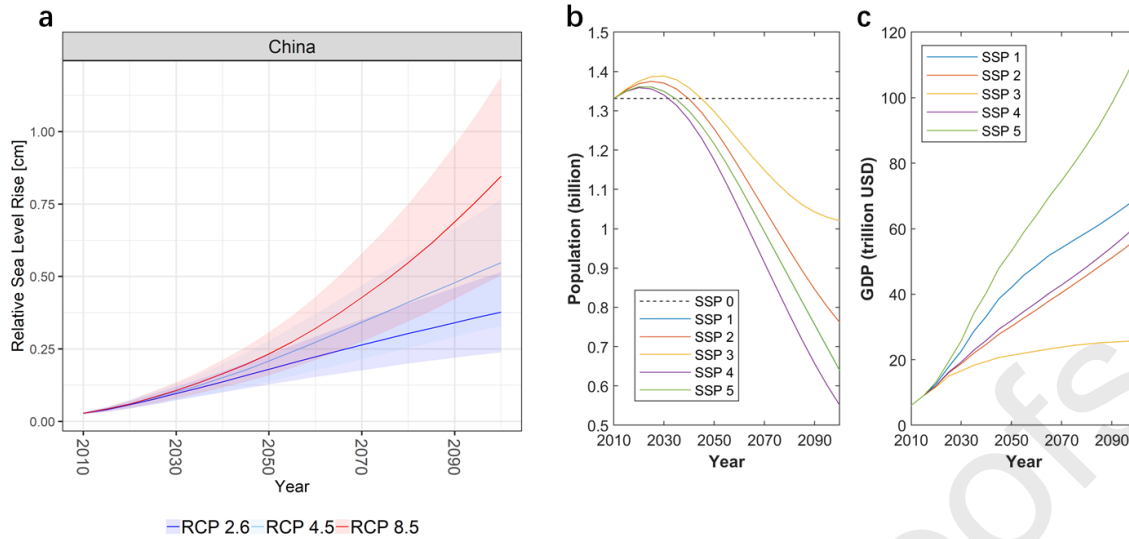
378

379 Fig. 1 Flowchart showing the general methodological approach by dividing into three steps.



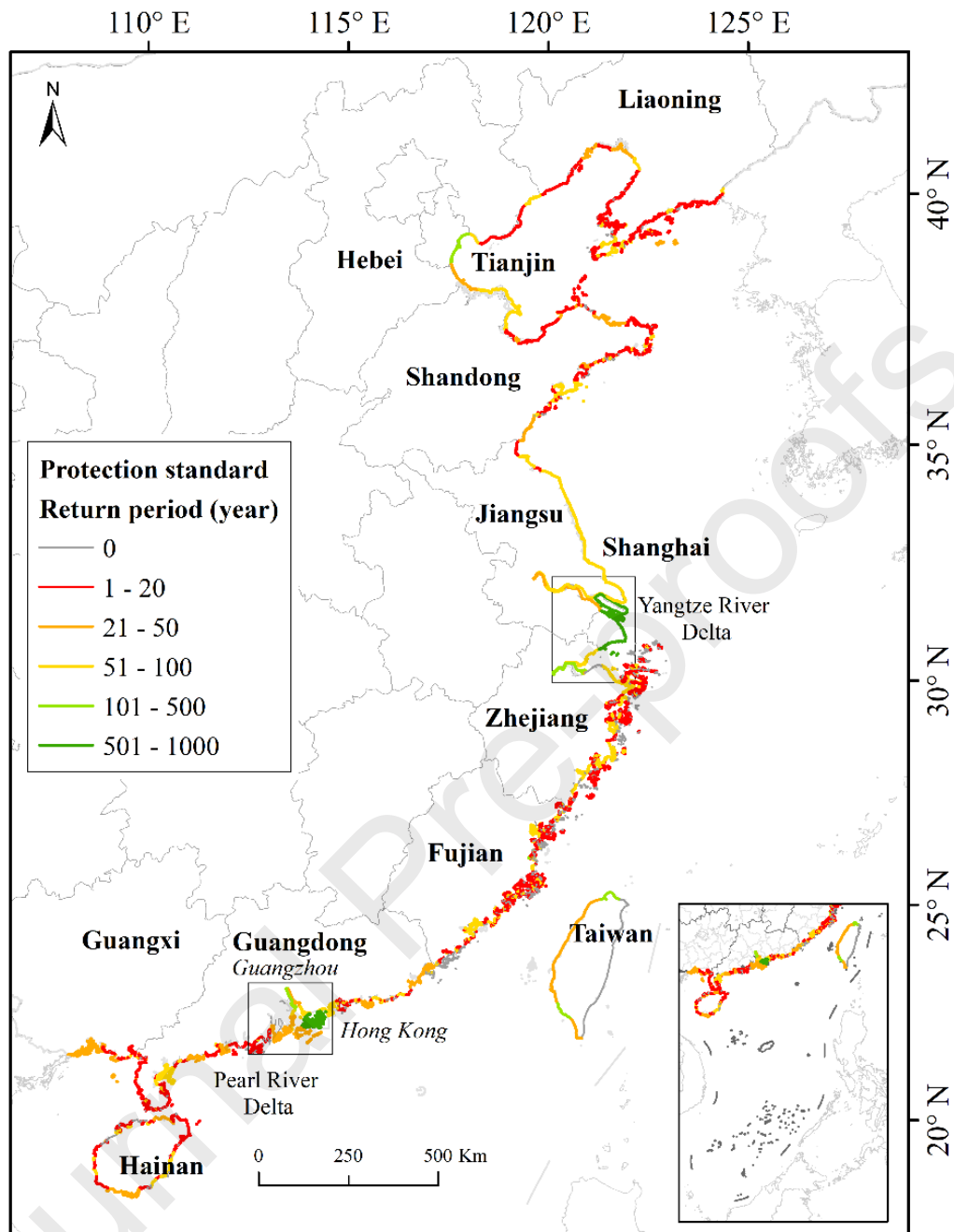
380

381 Fig. 2 Damage curve for the assessment of assets in the DIVA flood module (Blue line shows
 382 an example of a 3 m of defence, the loss ratio over 3 m is same as without protection).



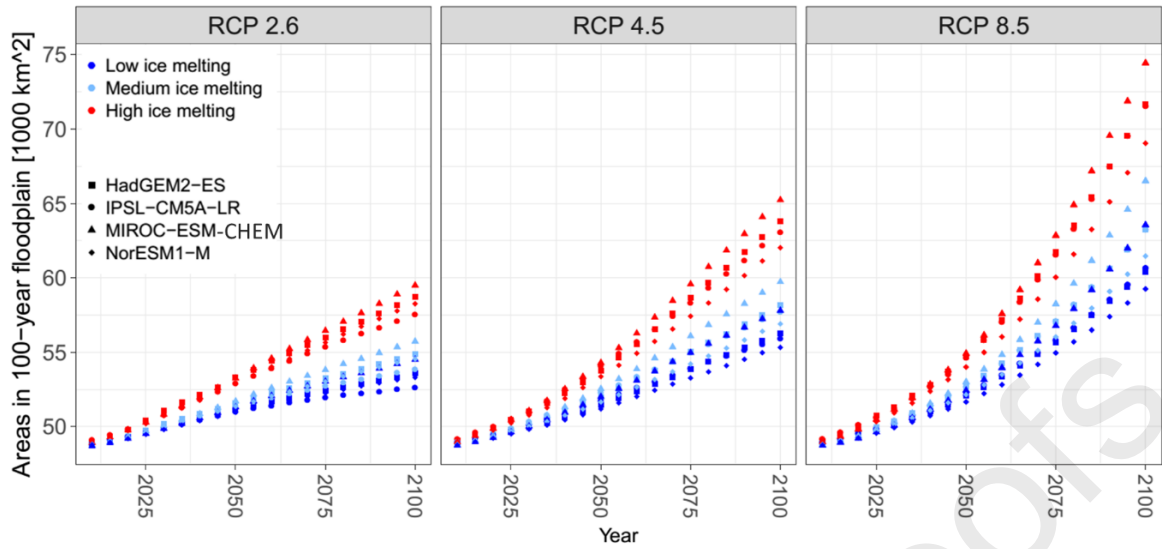
383

384 Fig. 3 a) The mean relative sea-level rise for China under sea-level rise scenarios (reference
 385 period: 1985-2005; Lines refer to median values, and shades areas show ranges of maximum
 386 and minimum values); b) Population (SSP5 overlays SSP1 for population, SSP0 only refers
 387 to no change of population); c) GDP of China for socio-economic scenarios from 2010 to
 388 2100.



389

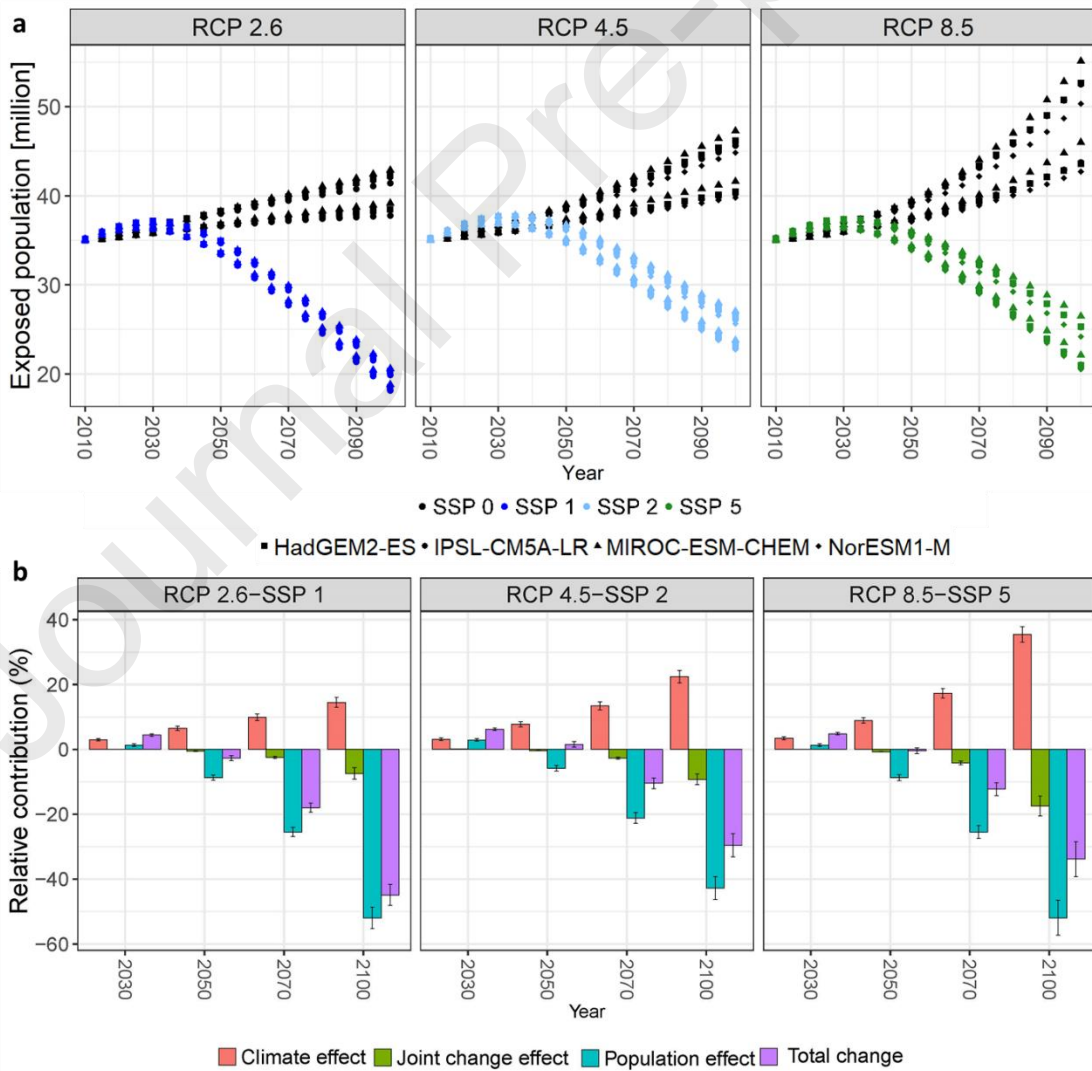
390 Fig. 4 Coastal protection standard (return period) of China.



391

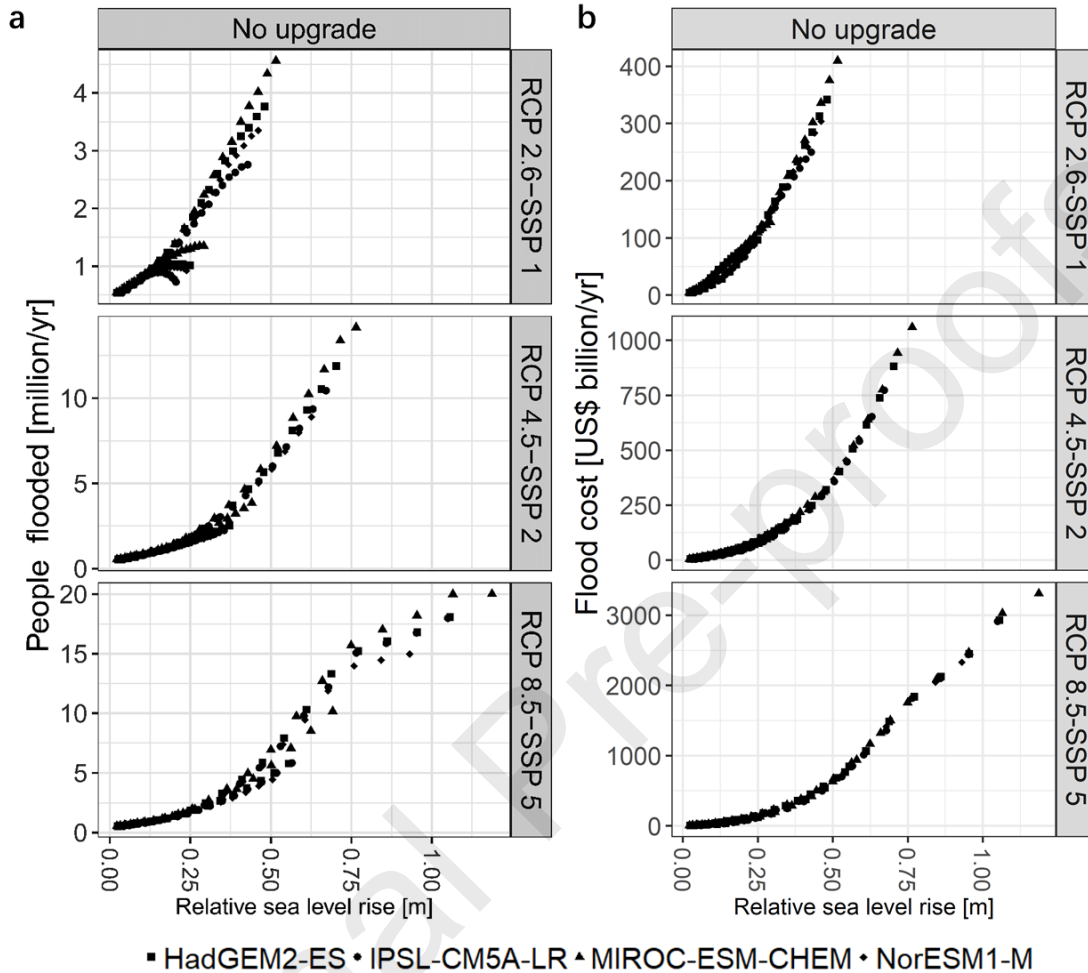
392 Fig. 5 Areas of the 100-year coastal floodplain over the 21st century under SLR scenarios.

393



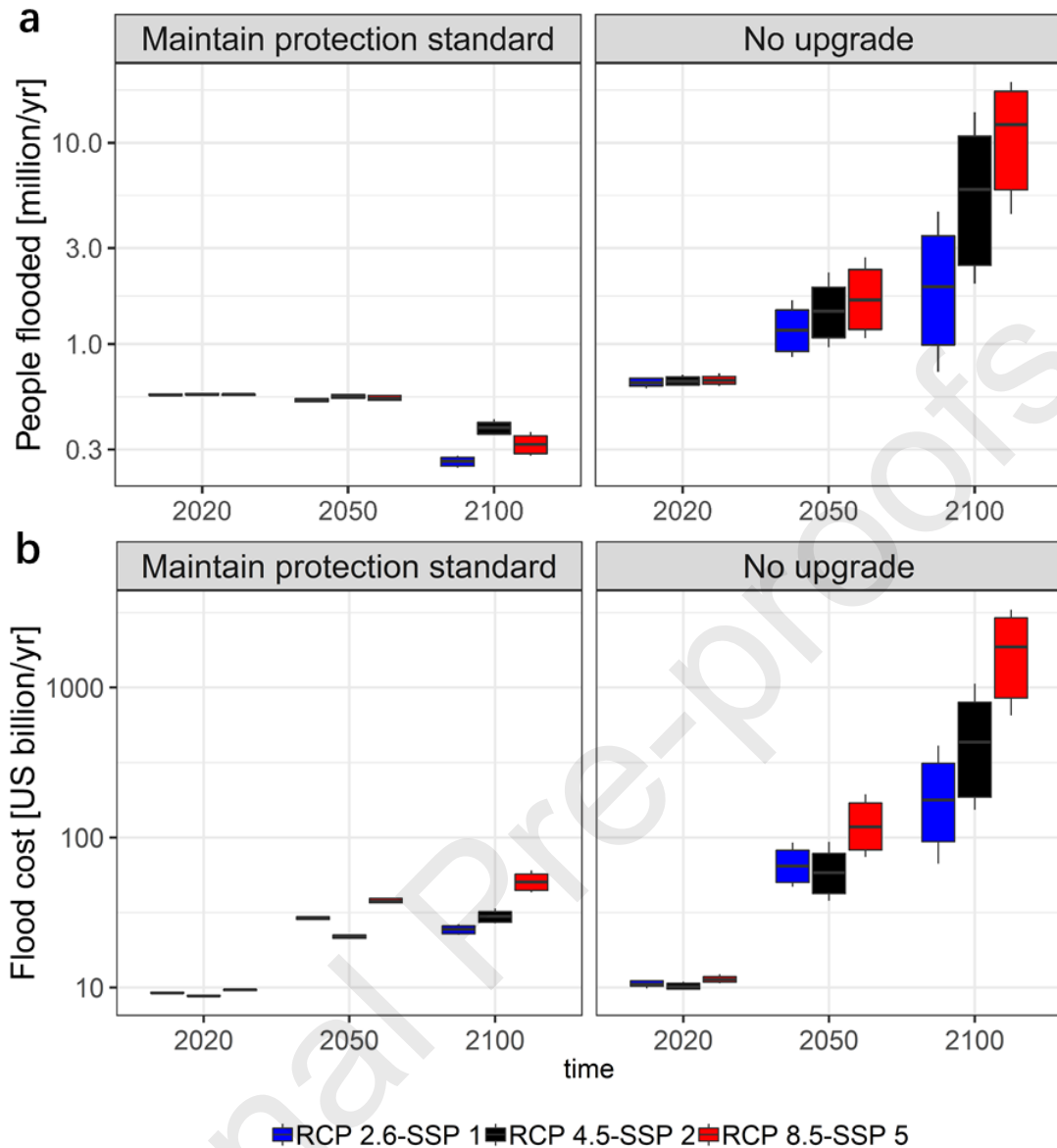
394

395 Fig. 6 a) Population below 100-year coastal floodplain under RCP-SSP scenarios in the 21st
 396 century; b) Relative contribution of changes to exposed population (below 100-year coastal
 397 floodplain) under SSP-RCP scenarios. Error bars illustrate the standard deviation in total
 398 exposure change across scenarios for each effect.



399

400 Fig. 7 People flooded and flood cost of China with relative sea level rise in the 21st century
 401 under a no upgrade to adaptation strategy with respect to 2010.



402

403 Fig. 8 People flooded and flood costs in 2020, 2050 and 2100 under two adaptation strategies.

404 On each box, the central mark indicates the median, and the bottom and top edges of the box

405 indicate the 25th and 75th percentiles, respectively. The whiskers extend to the most extreme

406 (maximum and minimum) data points.

407

408

409 Tab. 1 Length of China's coastline according to the coastal typology classification based on the high-
 410 resolution segmentation.

Coastal type	Coastline (km)	Percent (%)
Sandy	2703	9.3
Rocky	9577	33.0
Muddy	1722	6.0
Artificial coasts	14828	51.2
River mouth	137	0.5
Total	28967	100

411
 412
 413
 414
 415
 416
 417
 418
 419
 420
 421
 422
 423

Tab. 2 Coastline, artificial coastline, areas and population in the low elevation coastal zone (LECZ) areas ($DEM \leq 10$ m) in the first-level administrative divisions of China.

Province	Coastline (km)	Percent of national coast (%)	Artificial coastline (km)	Percentage of artificial coast to provincial coasts (%)	Territory (km ²)	Areas of LECZ (km ²)	LECZ to territory (%)	Total provincial population (million)	Populati in LEC (millio
						AW3D30			LandSc
Liaoning	2620	9.1	1685	64.3	135,916	12,262	9.0	44.7	6.2
Hebei	376	1.3	307	81.6	176,101	17,663	10.0	71.5	7.8
Tianjin	125	0.4	123	98.7	10,985	9,866	89.8	10.6	9.4
Shandong	2838	9.8	1735	61.1	148,269	21,031	14.2	96.1	8.6
Jiangsu	1247	4.3	1177	94.4	99,227	66,532	67.1	78.1	51.5
Shanghai	635	2.2	631	99.4	6,811	6,458	94.8	17.7	14.7
Zhejiang	6135	21.2	2287	37.3	103,621	16,005	15.4	49.0	21.9
Fujian	5042	17.4	1923	38.1	127,161	3,540	2.8	36.4	6.8
Guangdong	5344	18.5	2758	51.6	191,334	20,243	10.6	91.3	33.3
Guangxi	1299	4.5	890	68.5	252,891	1,623	0.6	46.9	0.9
Hainan	1647	5.7	190	11.5	38,762	2,554	6.6	8.1	1.9
Hong Kong	653	2.3	483	74.0	1,229	186	15.1	7.0	1.4
Macau	59	0.2	52	87.9	37	12	32.7	0.4	0.2

Journal Pre-proofs

Taiwan	947	3.3	586	61.9	103,621	2,942	2.8	23.0	4.6
Total	28967	100	14828	51.2	1,395,966	180,916	13.0	580.8	169.2

Journal Pre-proofs

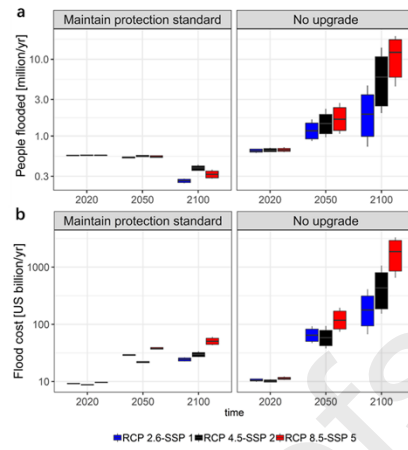
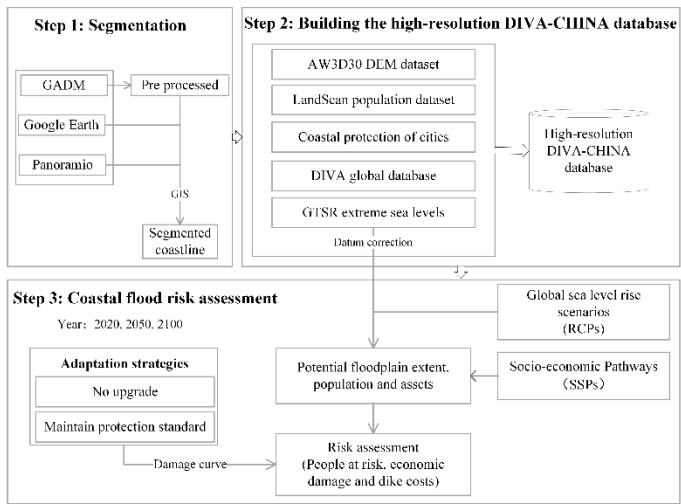
424 Tab. 3 Dike and flood costs in 2100 under multiple scenarios (The median and, in parentheses, the
 425 maximum and minimum values are provided. In the last two columns, the median value is considered
 426 to calculate reduced flood costs and increased dike costs).

SP	Flood costs (US\$billion/yr)		Dike costs (US\$billion/yr)		Reduced flood costs	Inc dike
	No upgrade	Maintain protection standard	No upgrade	Maintain protection standard		
CP2.6-SSP1	210 (67, 410)	24 (22, 26)	6 (4, 7)	9 (8, 10)	186 (45, 383)	3 (
CP4.5-SSP2	521 (153, 1060)	30 (28, 34)	4 (2, 6)	10 (9, 12)	491 (126, 1026)	6 (3
CP8.5-SSP5	1916 (650, 3308)	51 (43, 60)	2 (0.1, 5)	14 (11, 17)	1865 (607, 3248)	12 (

427

428

429



430

431

Journal Pre-proofs

432 **Highlights**

- 433 ● A refined coastal database of China is developed under DIVA framework.
- 434 ● Potential damage and adaptation costs of coastal flooding in China is quantified.
- 435 ● Maintaining constant protection reduces impacts by about one order of magnitude.
- 436 ● Dike costs are two orders of magnitude smaller than flood costs across all scenarios.
- 437 ● SLR is important to China with high potential impacts and adaptation needs.

438